UNITED STATES AIR FORCE

AIR UNIVERSITY

AIR FORCE INSTITUTE OF TECHNOLOGY

Wright-Patterson Air Force Base, Ohio

(1)

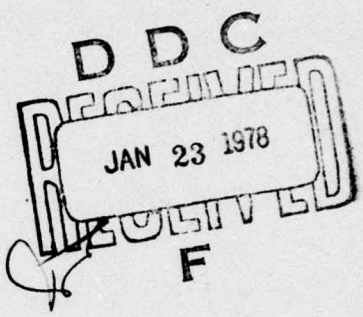

DEPTH-RESOLVED CATHODOLUMINESCENCE OF CARBON IMPLANTED GALLIUM ARSENIDE

THESIS

Martin J. Walter
2 Lt USAF

GEP/PH/77-15

Approved for Public Release; Distribution Unlimited.

(14) AFIT/GEP/PH/77-15

(6) DEPTH-RESOLVED CATHODOLUMINESCENCE OF CARBON IMPLANTED GALLIUM ARSENIDE.

(9) Master's THESIS

Presented to the Faculty of the School of Engineering

of the Air Force Institute of Technology

Air University

in Partial Fulfillment of the

Requirements for the Degree of

Master of Science

by

(10) Martin J. Walter
2 Lt USAF

Graduate Engineering Physics

(12) 68p. (11) Dec[illegible] 1977

Approved for public release; distribution unlimited.

PREFACE

In the completion of this thesis there were many people who assisted me. First, I would like to thank my advisor, Dr. R.L. Hengehold, who interested me in this thesis. His suggestions and the discussions I had with him were a great aid. I would also like to thank Major Bruce J. Pierce who aided me in understanding several points. I am grateful for the fine technical assistance and advice given me by Jim Miskimen, George Gergal, and Ron Gabriel of the AFIT Physics Laboratory staff. I would also like to thank Major Gary E. Vice with whom I had many discussions which clarified the material.

Martin J. Walter

TABLE OF CONTENTS

TABLE OF CONTENTS
(continued)

LIST OF TABLES AND FIGURES

LIST OF TABLES AND FIGURES
(continued)

ABSTRACT

The effects of two caps, SiO_2 and Si_3N_4, are examined on Cr doped GaAs by means of depth resolved Cathodoluminescence. The GaAs samples had been implanted with C^+ in fluences of 10^{13} cm^{-2} and 10^{14} cm^{-2}. Two of the samples differed only in the cap used.

The energy shift in the carbon-carbon, donor-acceptor, recombination, and the free-bound, carbon acceptor transition peak are used to evaluate the carbon donor, and carbon acceptor concentrations. These concentrations are used to evaluate the effects of the caps.

It is found that the carbon substitutes for both Ga and As; and that the Si_3N_4 cap permits greater outdiffusion of As than the SiO_2 cap; and that the SiO_2 permits greater outdiffusion of the Ga than does the Si_3N_4 cap.

DEPTH-RESLOVED CATHODOLUMINESCENCE OF CARBON IMPLANTED GALLIUM ARSENIDE

I. INTRODUCTION

The United States Air Force is interested in semiconductor devices which operate well in a high temperature environment. New device applications are awaiting the development of semiconductors with the appropriate electrical properties. Gallium arsenide with proper doping should have the desired properties.

Gallium arsenide (GaAs) is a semiconducting III-V compound. It has the zincblende crystal structure like many other III-V compounds. Its physical properties are similar to the group IV semiconductors silicon (Si) and germanium (Ge). The majority of differences between GaAs and the group IV semiconductors can be attributed to the partially ionic bond in GaAs (Ref. 14:371-2).

One method for introducing a dopant into GaAs is ion-implantation. The implantation introduces a dopant concentration profile which can be made sharper than with diffusion techniques. Implantation also introduces a good deal of damage which can be removed through annealing the crystals at temperatures near 800°C. However, at temperatures near 600°C, decomposition of GaAs is significant. To protect the surface,

and resist diffusion of the crystal elements, a cap of either Si_3N_4 or SiO_2 is placed on the sample.

The purpose of this experiment is to obtain depth-resolved cathodoluminescence from GaAs crystals which were doped with Cr, then implanted with carbon ions; and compare the spectra from a Si_3N_4 capped crystal with that of a SiO_2 capped crystal.

The theory of this thesis is discussed through Luminescence Mechanisms, their variations with concentrations, ion implantation, and electron beam penetration. The experimental part of this thesis deals with the cathodoluminescence apparatus, sample preparation, and procedures. The results are discussed by identification of transitions, analysis of depth resolved data, and analysis of the different caps. Finally some conclusions are drawn from these observations.

II. THEORY

The technique of implant profiling by depth resolved cathodoluminescence involves the excitation of luminescence from a sample which possesses an impurity profile, by means of an energetic electron beam. One must, therefore, understand luminescence and luminescence mechanisms; the variations of luminescence with concentration; how the impurity profile is introduced; and how the luminescence is excited by the electron beam.

This section will discuss these areas in the following manner: luminescence and radiative recombination mechanisms; the effects of concentration on luminescence; ion implantation of impurities; the penetration of an electron beam; and work that has been done on ion implanted GaAs, particularly carbon implants in GaAs.

Luminescence

The electro-magnetic radiation emitted when electron-hole pairs in a semiconductor recombine radiatively is called luminescence. In this section radiative recombination mechanisms are discussed with attention given to the effects of temperature and excitation intensity. These mechanisms include Band-Band, Band-Impurity, Impurity-Impurity, and Exciton. They are depicted in Figure 1.

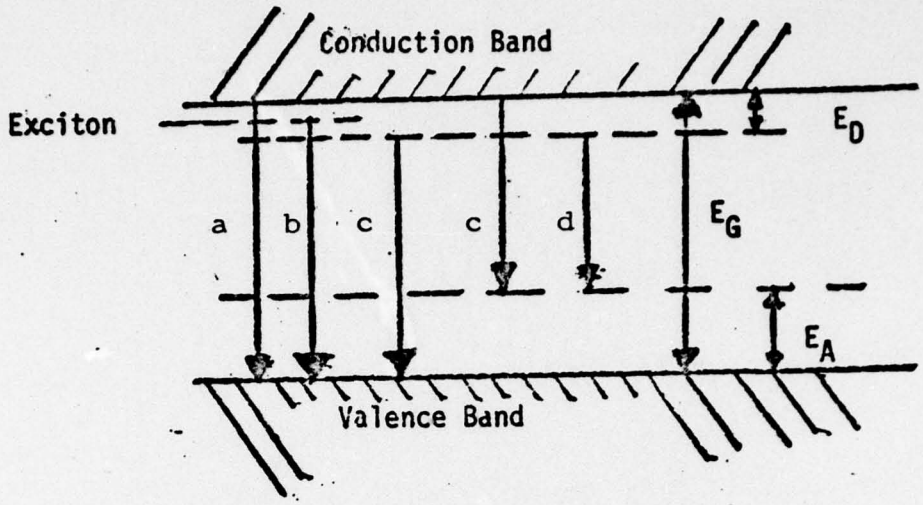

Figure 1: Luminescence Mechanisms; a.)band-band, b.) exciton annihilation, c.) free-bound, d.) bound-bound.

When an electron in the conduction band recombines with a hole in the valence band, the energy of the transition is the band gap energy (Eg = 1.519ev). However, this transition is not very probable and is rarely observed (Ref. 17:13).

Free-Bound Transition

When a "free" electron/hole recombines with a hole/electron which is bound to a simple impurity center such as a substitutional acceptor/donor the energy of the emitted photon,

E, is given by

$$E = E_g - E_i + \overline{E_K} \pm nE_p$$

Where; E_g is the band gap energy, E_i is the donor or acceptor energy level, $\overline{E_K}$ is the average kinetic energy of the electron/hole, E_p is the phonon energy, and n is any positive integer or zero.

In GaAs, these transitions can be distinguished by the energy of the transition because the donor level is very close to the conduction band ($\sim$6meV), while the acceptor level is deeper ($\sim$30meV) (Ref. 2:327-9).

Impurities with large ionization energies and defects such as vacancies and complexes from deep impurity levels (Ref. 16:139).

As the temperature of the semiconductors rises, $\overline{E_K}$ increases and the dispersion in energy increases, thus broadening the peak. This transition dominates at higher temperatures because the thermal energy depopulates bound exciton and shallow donor levels (Ref. 17:22). Since $\overline{E_K}$ increases with temperature the transitioning electron/hole is father into the band at higher temperatures than at lower temperatures. But, since the band gap energy decreases with increasing temperatures, the energy of the emitted photon will also decrease but not to the same amount as the band gap because of the $\overline{E_K}$ of the electron/hole.

Bound-Bound Transition

When a bound electron at a donor site recombines with a bound hole at an acceptor site, the energy of the transition is given by

$$E = E_g - E_A - E_D + \frac{e^2}{kr} \pm nE_p$$

Where; E_A is the acceptor level energy, E_D is the donor level energy, and $\frac{e^2}{kr}$ is the coulomb interaction between the donor and acceptor (Ref. 7:13). This shows that near pairs (r small) emit higher energy photons than far pairs (r large) whose energy is closer to the difference in E_A and E_D.

The radiative recombination rate goes as the inverse exponential of the separation of donors and acceptors. Hence, more distant pairs are saturated earlier than nearer pairs and an increase in intensity shifts the peak to higher energy. As the temperature is increased farther pairs become thermally ionized before recombination occurs, again shifting the transition energy to higher values (Ref. 7:85).

Exciton Transitions

Excitons can be viewed as electrons bound to holes in a hydrogen-like fashion. Exciton energy states lie very close in energy to the conduction band edge because, like the hydrogen atom, the exciton binding energy is proportional to the effective mass of the exciton which is very small.

Excitons may be free or bound. Bound excitons are associated with impurity sites in the lattice, where their energy is lower than that mentioned above by the energy required to bind the exciton to the site. Bound excitons are usually observed only at very low temperatures ($<20^{\circ}K$) because the rate of trapping carriers decreases with increases in temerature. Some characteristics of bound exciton transitions are narrow line shape ($\sim$0.1meV) and an intensity which decreases with increased temperature (Ref. 17:16-18).

Free excitons, on the other hand, move through the lattice and, therefore, have an additional kinetic energy above that mentioned earlier. They can exist in sufficiently pure materials and have line widths broader than the bound excitons ($\sim$1.meV) (Ref. 16:12-14).

Concentration Dependence on Luminescence

The banding of electronic energy states in a solid is the result of the overlap of the electronic wave functions. Likewise, when the concentration of an impurity reaches the level where the electronic wave functions of the impurities overlap, the impurity level will band. This banding has been shown to cause a shift in free-bound and bound-bound luminescence peaks. For simple hydrogenic n-type GaAs the carrier concentration at

which banding occurs is near $5x10^{16}cm^{-3}$, whereas for p-type GaAs, banding does not start until a concentration near $5x10^{17}cm^{-3}$ is reached. When the concentration reaches a higher level the impurity band merges with the crystal band; i.e., donor band into conduction band, or acceptor band into valence band. For n-type GaAs this occurs near a concentration of $1x10^{17}cm^{-3}$. However, p-type GaAs does not merge until the concentration is on the order of $2x10^{17}cm^{-3}$ (Ref. 2:358). This banding of a level and merger with a band is schematically depicted in Figure 2 (Ref. 4:14) for the acceptor level.

The hydrogenic donor levels band at a lower concentration than the hydrogenic acceptors because the donor electrons are bound much less tightly ($\sim$ a factor of 6) than the acceptor holes. Hence the wave function of the donor extends farther and interaction occurs at lower density.

Under increasing n-dopant concentration the donor-valence band transition energy in uncompensated material can be considered "band-band". The rapid rise of the transition energy shown in Figure 3 indicates the involvement of conduction band states (Ref. 6: 354). With increasing p-type concentration the conduction band-acceptor transition energy progresses to "band-band". However, a growing percentage of the luminescence

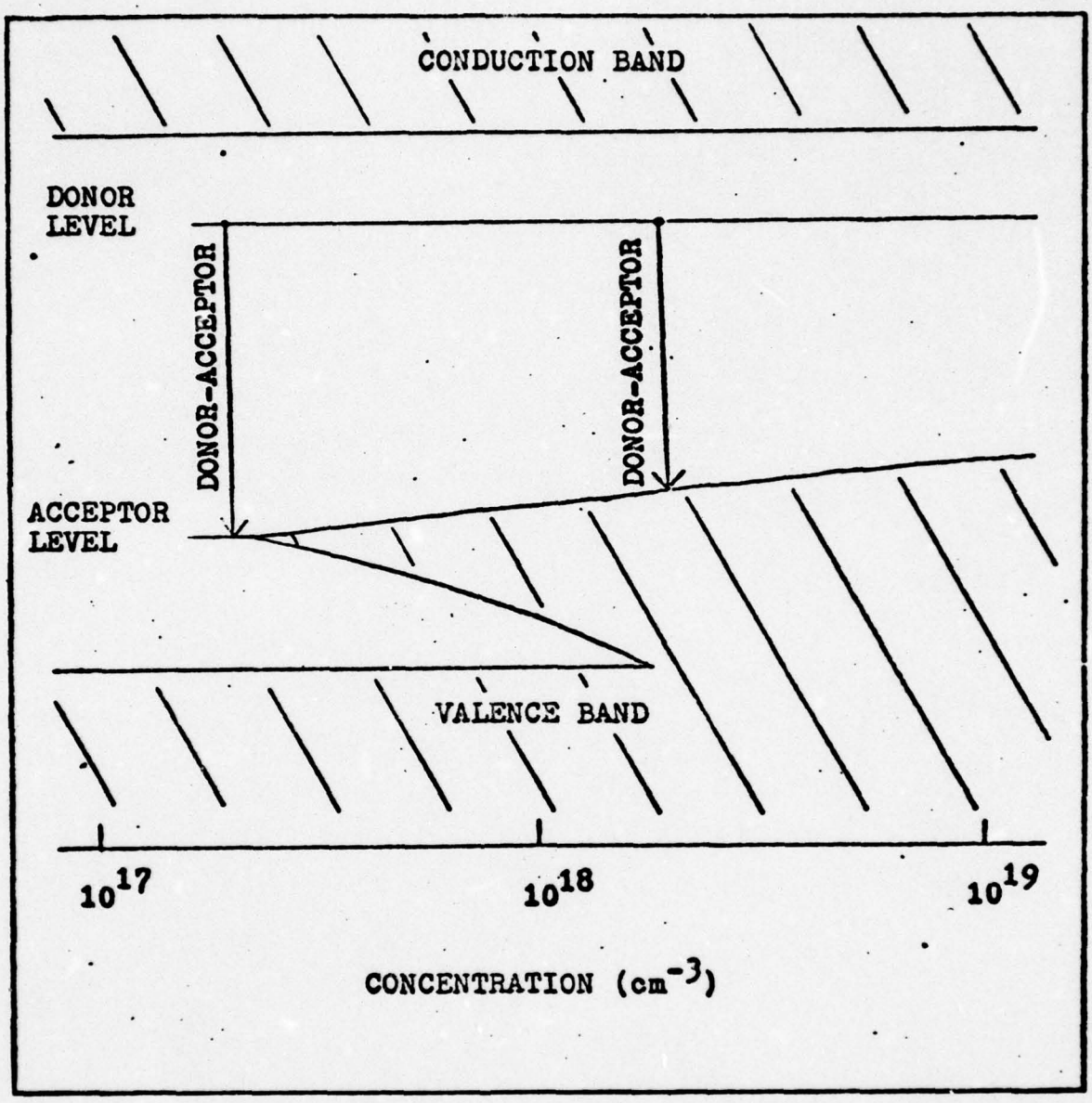

Figure 2. Schematic of Acceptor Level Banding (Ref. 4)

is attributable to donor-acceptor transitions from residual donors, which are acting to compensate the p-type acceptors. The variation of band-acceptor transitions in p-type GaAs as a function of carrier concentration is also shown in Figure 3 (Ref. 6:354-5).

In Figure 4 (Ref. 16) linebroadening of Zn doped p-type GaAs is shown as acceptor concentration is increased. This broadening is due to the broadening in the density of states at the acceptor level. Instead of a delta function-like density of states, the banding of the acceptor level has induced a density of states similar to that of either the conduction or valence band.

In highly compensated p-type GaAs the donor concentration can be high enough to induce banding of both donor and acceptor levels, since the donor level bands with an order of magnitude lower concentration than the acceptor level. This would lead to a decrease in donor-acceptor transition energies with increasing concentrations of donors and acceptors, as the donor level band would be empty at very low temperatures much like the conduction band in intrinsic material.

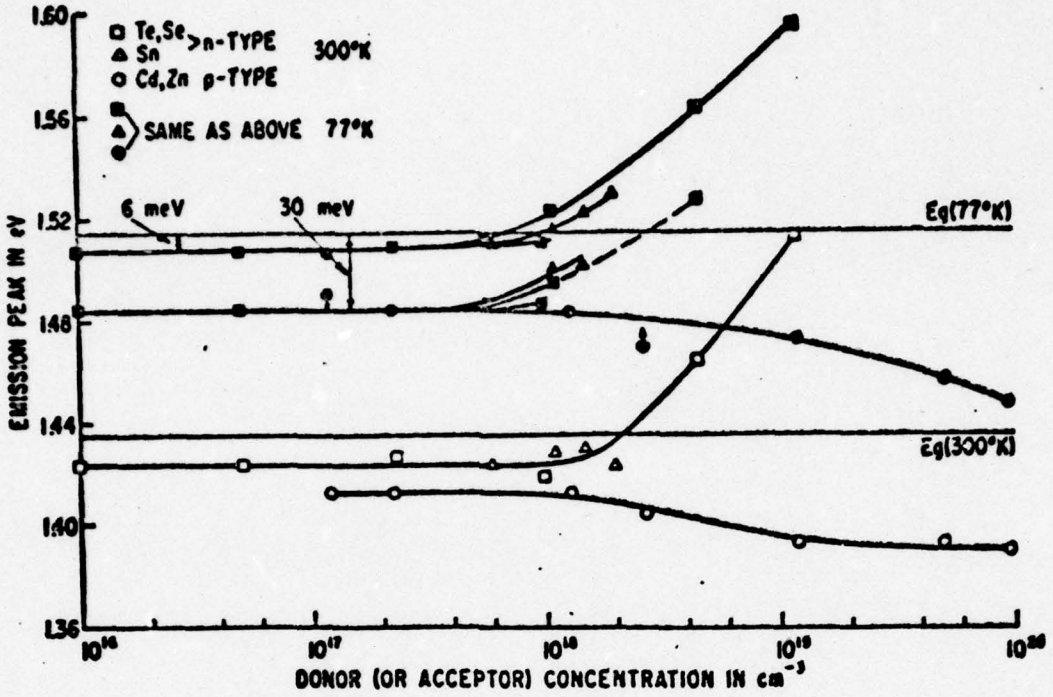

Figure 3: Dependence of Transition Energy on Doping (ref. 6)

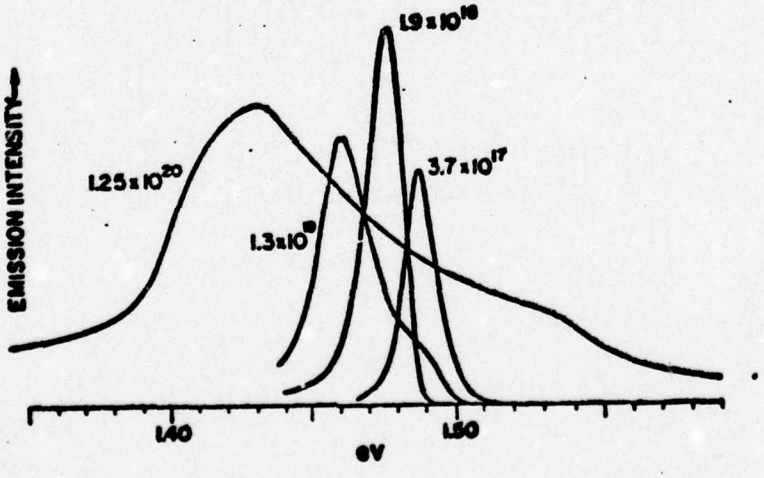

Figure 4: Dependence of Spectral Line Shape on Doping (Ref. 16)

Ion-Implantation

Ion-implantation is the technique of introducting ions into a substrate by using an energetic beam of ions. When a substrate is bombarded by a beam of energetic ions, some of the incident ions are implanted into the surface. However, host atoms are sputtered from the surface (Ref. 9:295). In this way desired impurities can be introduced into the substrate and the electrical properties can be altered to fit different applications.

As the ions move into the crystal, they interact collisionally with the electrons and nuclei in the crystal. Through these interactions the ions give up their energy and finally come to rest. These interactions, however, introduce damage into the crystal; first by sputtering the surface, and second by removing crystal elements and creating vacancies and interstitials. The second of these two is the more important as the periodicity and orderliness of the crystal is destroyed. The removal of this damage is necessary before electrical activity can be attained. This is accomplished through annealing of the sample, allowing interstitials to move to lattice sites and thus returning the periodicity to the crystal (Ref. 8:7).

The advantages that make ion-implantation worthwhile as compared to conventional doping methods include the ability to introduce precise concentrations of many impurities in three dimensions while avoiding high temperature problems associated with the diffusion method of doping (Ref. 4:2).

Although one avoids temperatures associated with diffusion techniques, annealing temperatures near 800°C are required to remove the lattice damage. This temperature is above the temperature at which substantial decomposition of the GaAs occurs (600°C). To resist this decomposition and the out-diffusion of the Ga and As, caps are placed on the surface. The effects of these caps are not understood well, and this work examines the effects of Si_3N_4 and SiO_2 as caps.

When the ions have come to rest, there will be a distribution of stopping points as a result of the random nature of the collisions and the energy transferred in each collision. This distribution is characterized by a mean ion range and standard deviation (Ref. 9:297). Lindhard, Schiott and Scharff have developed a theory which best describes the range distribution by using a gaussian function (Ref. 12:4).

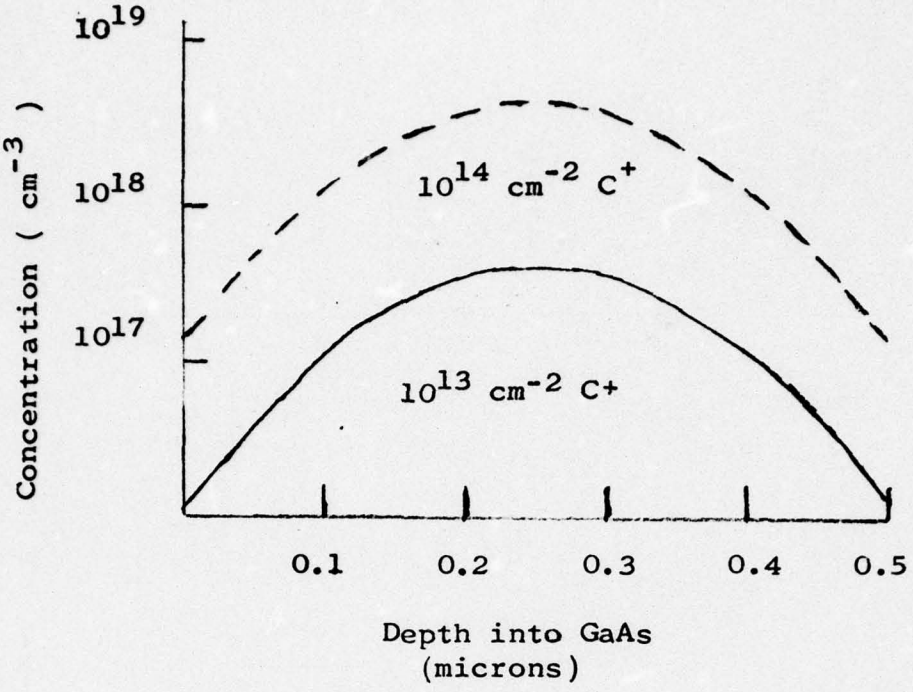

Figure 5: Projected concentration profile for 120KeV C+ implant.

Using this theory, the expected distribution of carbon prior to annealing is shown in Figure 5. The mean projected range for this distribution is 0.25 microns.

Electron Beam Penetration

When luminescence is induced by an impinging electron beam it is called cathodoluminescence. This technique offers the advantage of being able to produce electron-hole pairs at various depths in the material providing a non-destructive method for profiling ion implants.

As the electrons penetrate the crystal, they give up their energy over a range of depths creating electron-hole pairs. Martinelli and Wang (Ref. 13) have measured the depth to which the beam will penetrate as a function of beam energy.

The profile of this penetration into GaAs and other luminescent crystals has been discussed extensively (Ref. 4, 15, 18). The penetration profiles in Figure 6 (Ref. 4:12) assume the penetration depths of Martinelli and Wang (Ref. 13) are valid at 45° as well as normal incidence and are scaled to E_b/X_R in the fashion of Norris et al (Ref. 15), where E_b and X_R are the beam energy and penetration depth respectively.

Assuming these profiles to be accurate, the problem of specifying the depth of luminescence cannot be solved without taking into account the diffusion of the electron-hole pairs. The analysis of this problem was assumed to be beyond the scope of this thesis.

Previous Work

The work performed, previous to this thesis, on Ion Implanted GaAs has dealt primarily with Cd implants. Very little work has been directed toward carbon implants up to this point. The two works discussed here are AFIT master's theses investigating Cd implanted GaAs.

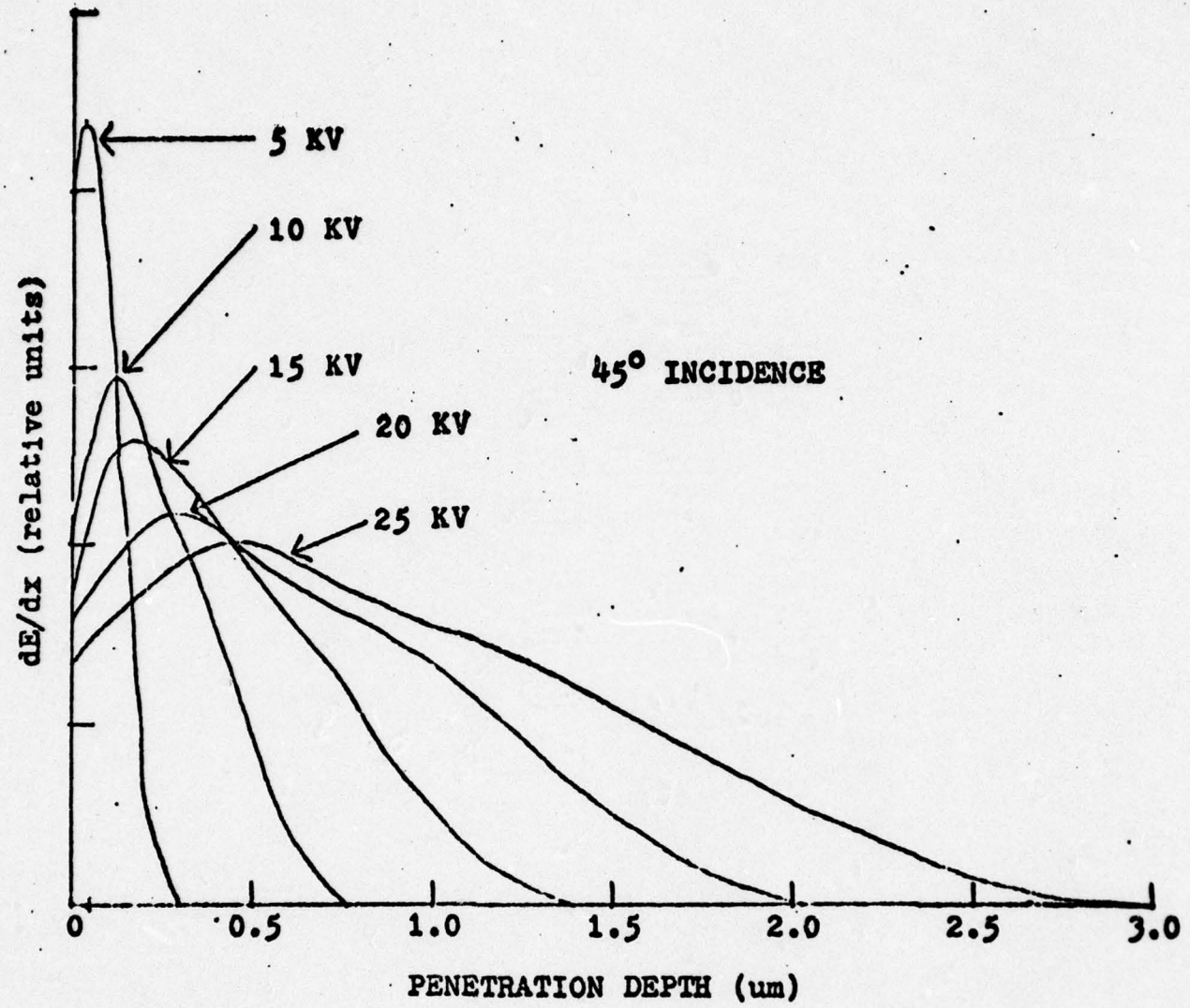

Figure 6. Estimated Electron Excitation Profiles in GaAs (Ref. 4)

Boulet (Ref. 4) made depth resolved cathodoluminescence measurements on cadmium implanted gallium arsenide. Using beam energies from 5 to 20 KV.a cadmium concentration profile was inferred from the spectra.

Dumoulin (Ref 8) studied the effects of implanting and annealing in GaAs using depth resolved cathodoluminescence. Unannealed samples were probed to find the extent of the damage layer induced. Several annealing temperatures were examined to find the temperature needed to remove the damage layer. It was concluded that the LSS profile did not predict very well the concentration profile after annealing of the samples.

III. EXPERIMENT

This section details the experimental work of this thesis. This is accomplished by describing the features of the experimental system needed to induce, detect, and process the luminescence data; by describing the preparation of the samples which were studied; and by describing the procedures used with the experimental system.

Electron Beam System

This system has not been used previously, but is similar to the system used by Dumoulin (Ref. 8). The electron gun is a Hughes Aircraft Company B-91-16A35 manufactured by their vacuum tube products division. The electron beam is controlled with five magnetic coils: alignment coil, centering coil, stigmator coil, focus coil, and deflection yoke.

As shown in Figure 7, the electron gun is located directly beneath the sample chamber; the beam moving vertically. The five coils are mounted on the column and are used to produce a focused beam at the sample.

The stigmator and focus coils are mounted together on a bracket which as five precision positioners which include: pitch, yaw, two horizontal translations, and rotation. These

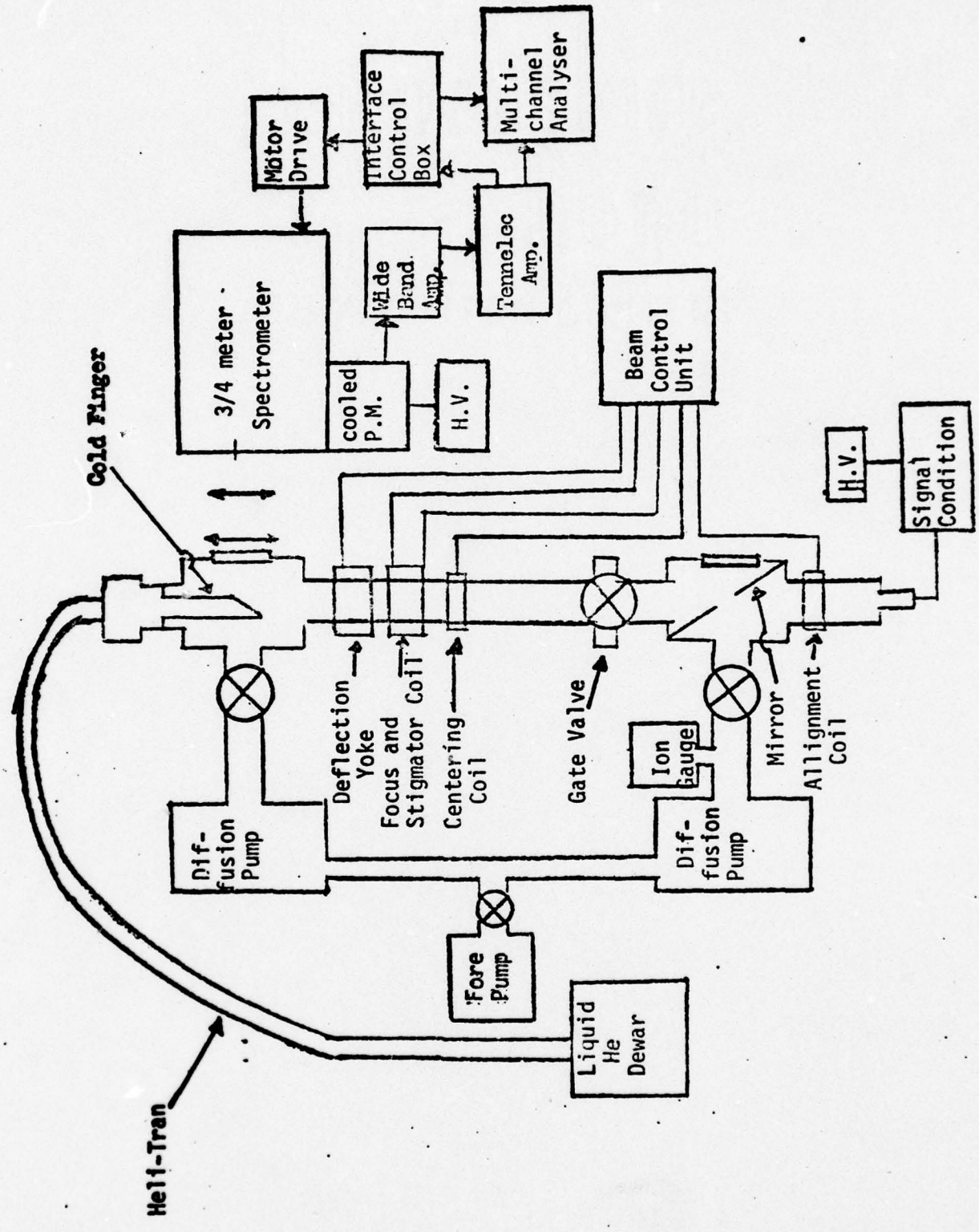

Figure 7. Cathodoluminescence System Diagram

allow the coils to be positioned so that an adjustment of the focus does not cause the beam to move on the sample. The deflection yoke is mounted on a similar bracket.

The vacuum is maintained by two diffusion pumps with a common mechanical forepump. The diffusion pumps are air cooled and the one closest to the sample chamber is equipped with a liquid nitrogen trap. The vacuum pressure was observed with a Veeco ionization gauge and an RG-83 ionization gauge control. However, the gauge was located far from the sample chamber, near the lower diffusion pump as can be seen in Figure 7. This position does not lend itself to an accurate measure of the sample chamber pressure.

Sample Mounting and Cooling

Four samples were mounted on the face of the cold finger, along with a faraday cup which was used to measure the electron beam current. Each sample was held in place by a copper mask with a circular hole, which exposed the sample beneath. A small amount of a liquid alloy, of Ga, In, Sn, was used as a thermal contact between the samples and the cold finger. The masks are described in detail by Boulet (Ref. 4). The cold finger was mounted vertically on two O-rings which permitted rotation of the finger while still maintaining the vacuum. The cold finger face was cut at a 45° angle from the

vertical electron beam and from the horizontal axis of the spectrometer.

The cold finger was cooled by the use of an Air Products Heli-Tran system. The Heli-Tran consists of three tubes; the outermost of these is a vacuum jacket. The next tube is a shield tube through which helium flows from the pressurized dewar to the cyro-tip and back to the dewar, exiting the Heli-Tran to a flow meter where flow can be monitored and restricted.

The innermost tube cools the cold finger. The helium flows into the cyro-tip cooling the sample mount. The gas is then vented through a flow meter. The helium flow can be controlled with a needle valve located in the cyro-tip of the Heli-Tran. The mounting of the cyro-tip is protected from extreme cold by a vent gas heater.

The dewar end of the Heli-Tran has a gas tight seal and dewar pressures near 10 psi were used for cooling, while pressures near 3 psi were used for running. The dewar end was equipped with a filter to keep debris from entering the Heli-Tran.

The temperature of the cold finger was monitored with a chromel vs. gold .07 atomic % iron thermocouple with a liquid nitrogen reference. The temperature was read in microvolts on a data precision 3500 digital voltmeter.

Luminescence Detection

The luminescence was examined by the use of a Spex 1702 3/4 meter Czerny-Turner spectrometer. The spectrometer was equipped with a 600 gr/mm grating, which was blazed to 1.6 micron. The entrance and exit slits were straight and independently adjustable from 6 micron to 3 mm. The luminescence was collected by a two lens system. The collecting lens had a 10 cm focal length and was mounted just outside the quartz window of the sample area. A lens of 20 cm focal length was used to focus the luminescence onto the spectrometer slit.

An RCA C70007A photo-multiplier tube with an S-1 response and cooled to -50°C by a Products for Research temperature controller was used to detect the luminescence. The high voltage applied to the photo-multiplier tube cathode was supplied by a Keithley 244 High Voltage Supply.

Signal Processing

The photo-multiplier tube converts the incident photons into a series of electrical pulses. These pulses are amplified by a wide band amplifier and then by a Tennelec amplifier, and are input for a Multi-Channel Analyzer (MCA). The MCA then counts these pulses into a channel. The channel selector of

the MCA is advanced at a specified rate with respect to the advancement of the spectrometer. In this way the incident photons within a specific wavelength band are counted, and the spectrum is digitized. This same system was used by Dumoulin (Ref. 8).

Sample Preparation

Samples one and two were taken from the same GaAs wafer which had been doped with Cr and implanted with 10^{13} cm^{-2} of 120 KeV carbon ions. Sample one was then capped with $\sim$1000Å Si_3N_4, while sample two was capped with $\sim$1000Å SiO_2. Both samples were then annealed at 850°C for 15 minutes.

Sample three was taken from a wafer of GaAs doped with Cr and implanted with 10^{14} cm^{-2} of 120 KeV carbon ions. It was capped with $\sim$ 1000Å Si_3N_4 and annealed for 15 minutes at 850°C. Another sample was cut from the same wafer and capped with $\sim$ 1000Å SiO_2. However, time did not permit the examination of this latter sample.

Sample four was implanted with 10^{13} cm^{-2} carbon ions at 120 KeV, then capped with $\sim$ 500Å Si_3N_4.

Procedure

In this section the procedures used during the experiment are detailed in four areas: mounting the samples, changing the gun, aligning the optics, and data collection.

Mounting the Samples. In order for the samples to be mounted, the cold finger must be removed from the vacuum system. This was done when the system was at room temperature and the Heli-Tran had been disconnected.

The sample chamber was isolated by means of the gate valve in the electron beam column and a Butterfly valve to the diffusion pump. It was then raised to atmospheric pressure by filling with dry nitrogen. The cold finger was withdrawn from the chamber and the hole was covered to keep dust from entering the system.

After the samples had been changed, the cold finger was placed in the chamber. The mechanical pump was used to rough down the chamber after being isolated from the diffusion pumps. When chamber pressure was near 15 microns of mercury the valve connecting the mechanical pump and chamber was closed. The valve between the diffusion pumps and rough pump was opened and shortly the Butterfly valve and gate valve were also opened.

Changing the Gun. When the electron gun cathode and filament needed to be replaced, the electron beam column as well as the sample area was raised to atmospheric pressure because the chamber has only one bleed in port and one rough pump connection, and both are in the sample chamber area.

With the system as noted prior to replacing the samples, the column was isolated from the diffusion pumps and filled with nitrogen. There was no power applied to the gun and the leads were removed. The gun was withdrawn and the filament and cathode were replaced. The gun was returned to the system, which was evacuated in a manner similar to that described above.

When the pressure had been reduced to operating levels, the cathode was aged by applying the voltages for the times listed in Table I.

TABLE I

Electron Gun Aging

Filament	Grid 1	Grid 2	Cathode	Time
	Volts			Min.
6.3	0	0	0	1
12.5	0	0	0	1½
9.0	5	150	0	10
9.0	0	0	0	10
6.3	0	0	0	5

Alignment of Optics. When the samples had been cooled and the helium flows had stabilized, a He-Ne laser beam was reflected off the mirror in the lower window onto the desired sample. The cold finger was rotated slightly until the reflection from the sample was near the spectrometer input slit. The electron beam was then placed on the sample and the lenses were positioned so that the red light struck the slit. The laser was turned off and the slits were opened to the maximum extent. The multi-channel analyzer was placed in the accumulate mode and the spectrometer was manually scanned to find a peak. Once the spectrometer was set on a peak, the lenses were adjusted so that the intensity of the light was maximized.

Data Recording. The beam energy was chosen and the beam was placed on the faraday cup. The beam current was then set by adjusting the grid voltages and when necessary, the filament current. The optics were aligned and the slits were closed to 100 microns, so that there was sufficiant resolution of the calibration line. The calibration lamp was set up and turned on. The multi-channel analyzer (MCA) was set to accumulate mode, the spectrometer was set to external drive, and the stepping drive, described by Dumoulin (Ref. 8) advanced the spectrommeter. When the spectrometer was approximately 5Å below the wavelength of the calibration line, the channel advance of the

MCA was started. After the calibration line had been recorded, the lamp was turned off and the slits were opened to a value from .5 to 1.mm. The spectrometer was scanned until all 1024 channels of the MCA had been scanned.

After each run a photograph was taken of the spectrum displayed on the oscilliscope, and a paper tape was made to record the counts in each channel. These tapes were then transcribed onto computer cards and plotted using the computer.

The optics were adjusted before each run as the collecting lens needed to be removed so that the electron beam could be visually adjusted to place it on the faraday cup and the next sample.

IV. RESULTS AND DISCUSSION

The results of this experiment will be discussed in three sections. First, the transitions associated with the observed luminescence peaks will be identified. Second, the depth resolved results will be discussed as they relate to the concentration profile. Finally, the results of the measurements on samples with different caps will be analyzed. As was mentioned earlier, higher energy electrons penetrate further into the crystal than lower energy electrons. Throughout this discussion, crystal depth will be designated by the electron beam energy.

Identification of Peak Transitions

Spectra obtained from sample one are shown in Figures 8, 9, and 10. These spectra exhibit six peaks with the highest energy peak lying at 1.509eV. This peak has been identified by Boulet and Bogardus (Ref. 4:30, 3:995) as unresolved exciton and donor-valence band transitions. The spectra in Figure 9 support this identification as this peak becomes more dominant with increased beam current and does not become saturated. The temperature variation shown in Figure 10 also supports this identification in that this peak becomes dominant at high temperatures and has shifted to lower energy by 10meV.

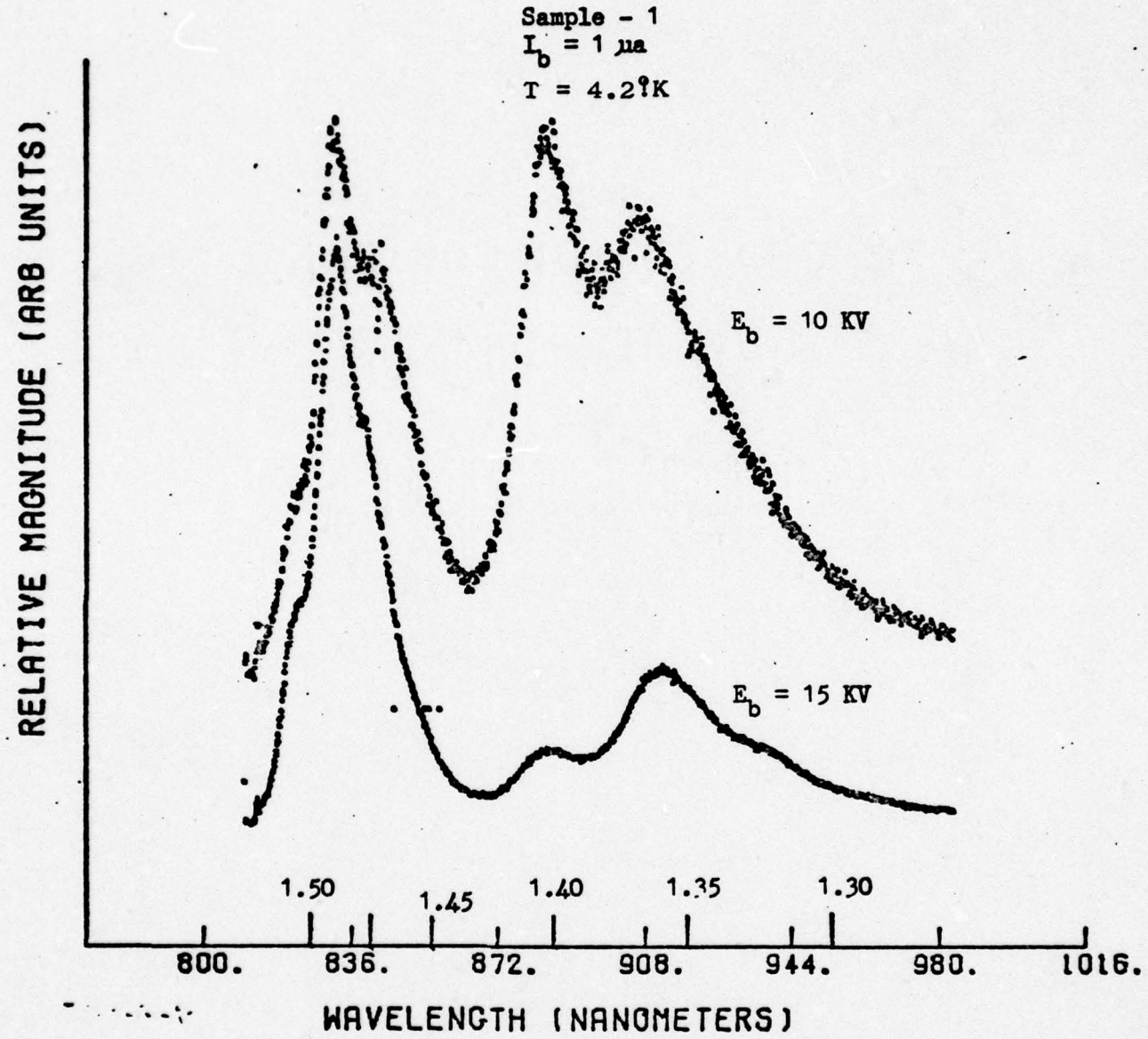

Figure 8. Typical Spectra for Sample One

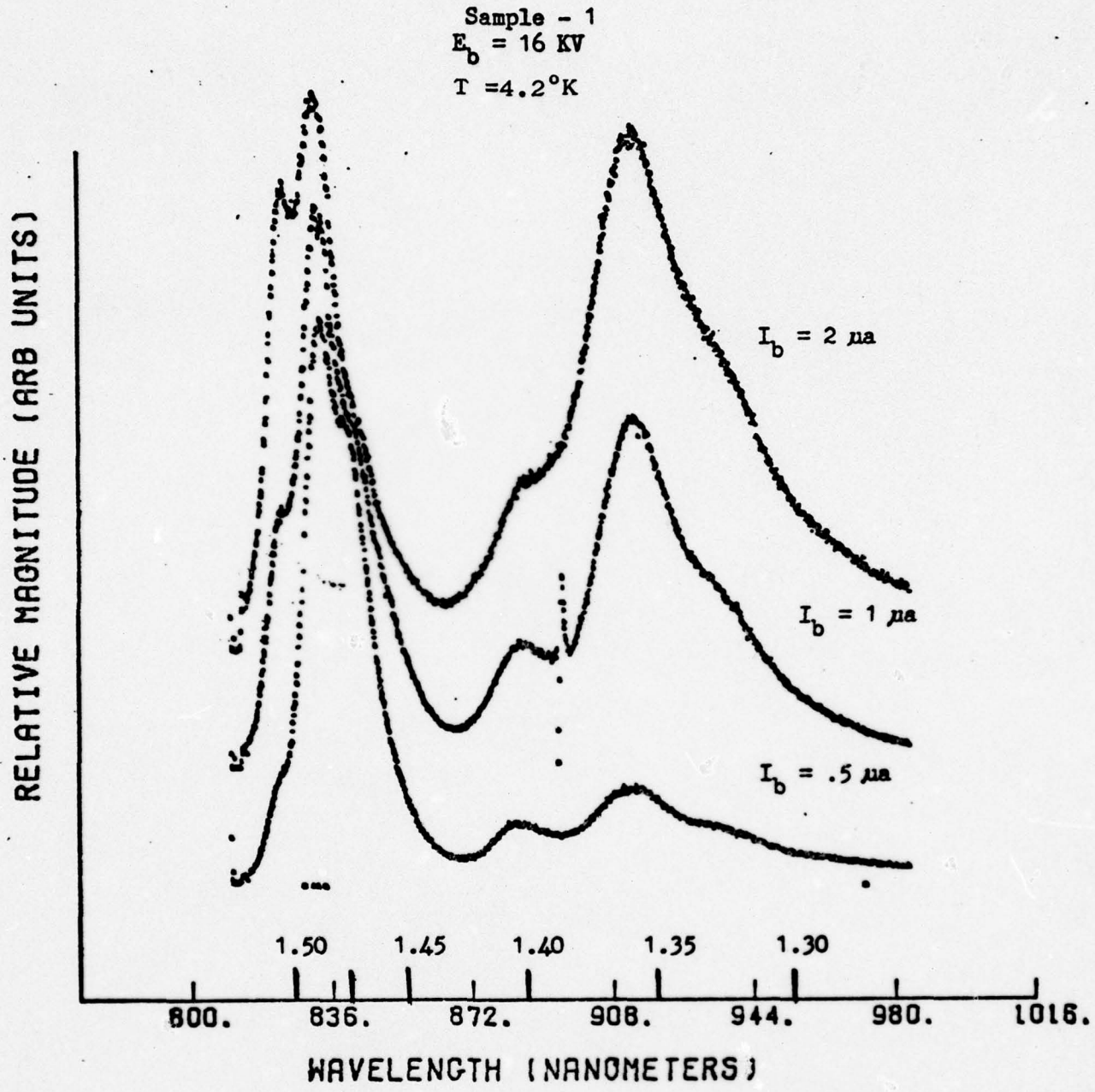

Figure 9. Beam Current Variations for Sample One

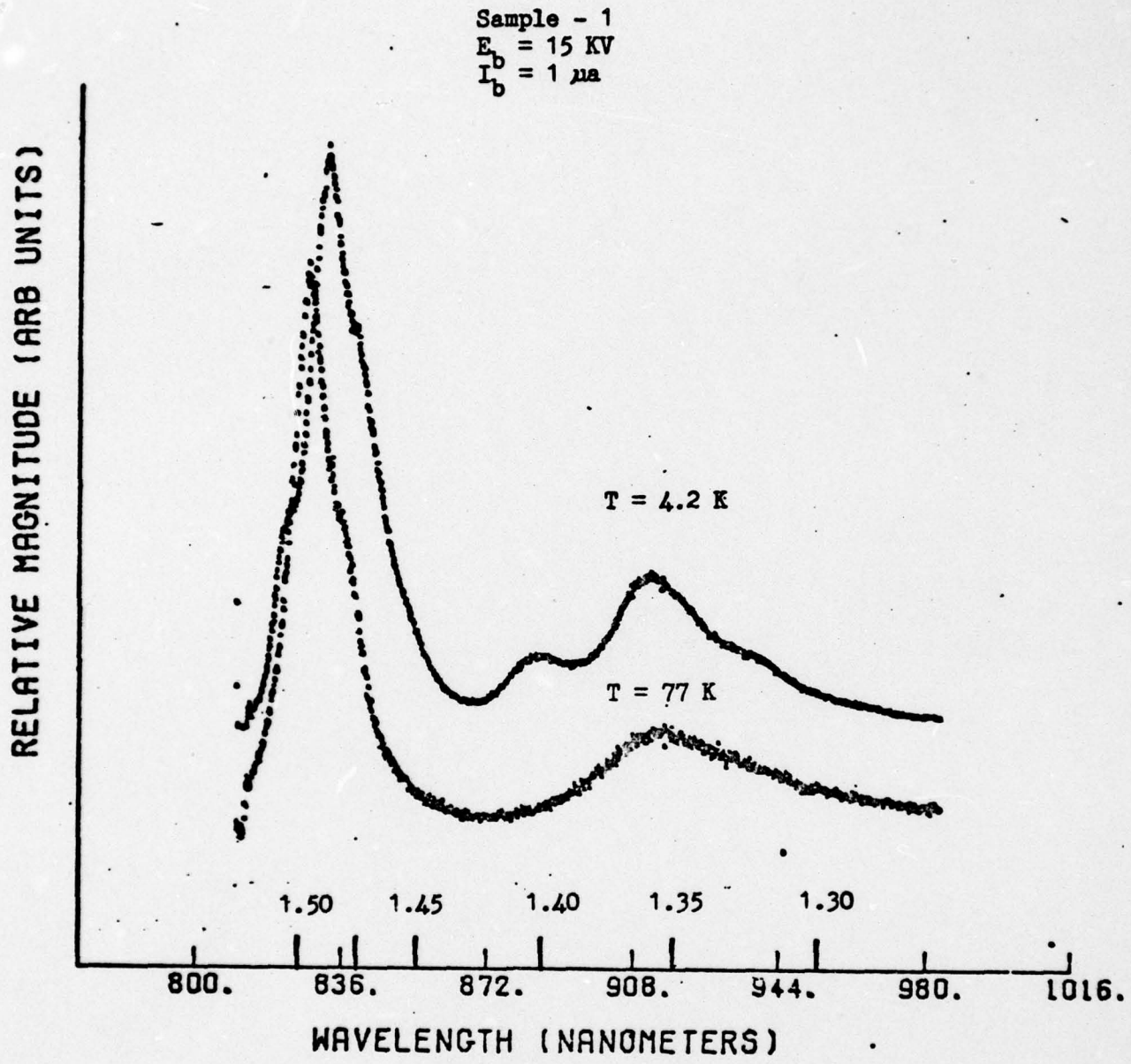

Figure 10. Temperature Variations for Sample One

The dominant peak in the spectra of Figure 8 has an energy of 1.491 eV. This is close to the expected acceptor transition using the data of Kamiya and Wagner (Ref. 11) and the values observed by Ashen *et al* of 1.492 eV. The variation of this peak with temperature is shown in Figure 10. At 77°K it is much less intense and has shifted to a lower energy. However, this shift is not as great as that of the exciton line. This indicates a free-bound transition and is identified as the conduction band-carbon acceptor transition.

The shoulder at 1.476 eV is close to the expected donor-acceptor transition in light of Kamiya and Wagner's acceptor energy (Ref. 11). In Figure 9 it can be seen that in the 2μa spectra this peak is substantially over-shadowed by the carbon acceptor transition indicating saturation of the transition. The 77°K spectra also shows that this peak gets washed out at higher temperatures. This behavior is indicative of donor-acceptor pair transition and is identified as a carbon-carbon (C-C) transition.

The peak at 1.404 eV exhibits the bound-bound transition characteristics of the previous transitions in Figure 9 and Figure 10. Itoh and Takeuchi (Ref. 10) have identified a peak near 1.40 eV as being due to an As vacancy - Si acceptor transition. Since the carbon acceptor level is near that of

Si (Ref. 11) it seems reasonable to identify this peak with the As vacancy - carbon acceptor transition.

The peak near 1.359 eV has been under some discussion in the literature. Chatterjee *et al* (Ref.5) have associated this transition with a Ga vacancy as a result of annealing studies. At 77°K as shown in Figure 10 this peak has shifted to lower energy within 1meV of the energy shift of the carbon acceptor free-bound transition (1.49 eV). An increase in beam current, as shown in Figure 9, shows this transition dominating the As vacancy - carbon transition. This probably indicates a free-bound transition. However, it should not be associated with the As vacancy since the bound-bound transition with the shallow carbon acceptor has a higher energy. Therefore, this peak is associated with a free-bound Ga vacancy transition.

The peak at 1.323 eV has also been identified with a Ga vacancy (Ref. 5:1422). This peak is washed out in the 2μa spectra shown in Figure 9. It is also absent in the 77°K spectra, indicating a bound-bound transition. Since gallium vacancies are acceptor sites and the 1.35 eV peak is free to bound, a donor with an energy level 33 meV below the conduction band is involved. Since Ga vacancy complexes with simple donors such as Si have been associated with a 1.2 eV emission

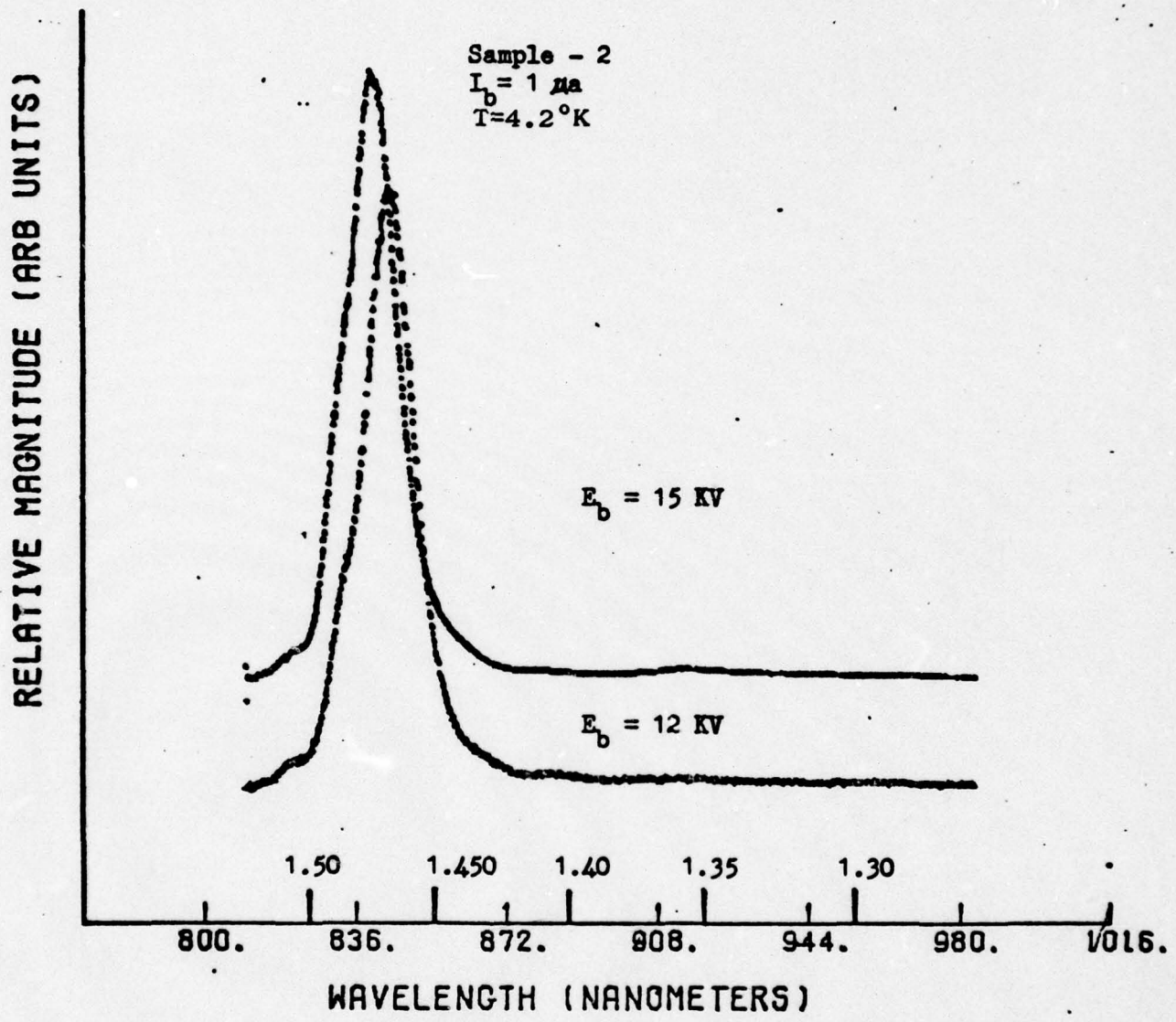

Figure 11. Typical Spectra for Sample Two

(Ref. 2:359-60) it cannot be associated with Ga vacancy complexes. Likewise the As vacancy associated with the 1.40 eV line is too deep. The possibility that this peak is associated with interstitial Ga exists since interstitial gallium is a donor; however, no reference of this was found in the literature. The peak at 1.323 eV is probably a donor-acceptor transition involving a Ga vacancy.

Typical spectra for sample two are shown in Figure 11. This spectra consists of six peaks described for sample one. These peaks can be attributed to the same transitions as those in sample 1. The 12 KV spectrum has significantly different energies for the transitions than the 15 KV spectrum. The shifting of these peaks will be discussed under depth resolved data.

Typical spectra for sample three are shown in Figure 12. The 12 KV spectrum consists of three peaks at 1.464 eV, 1.407 eV, and 1.364 eV. The 15 KV spectrum consists of six peaks. These six are again identified in the same way as those from sample one and can be associated with the same transitions. The three peaks in the 12 KV spectrum are identified as C-C at 1.464 eV; As vacancy-c at 1.407 eV; and free-bound Ga vacancy at 1.36 eV.

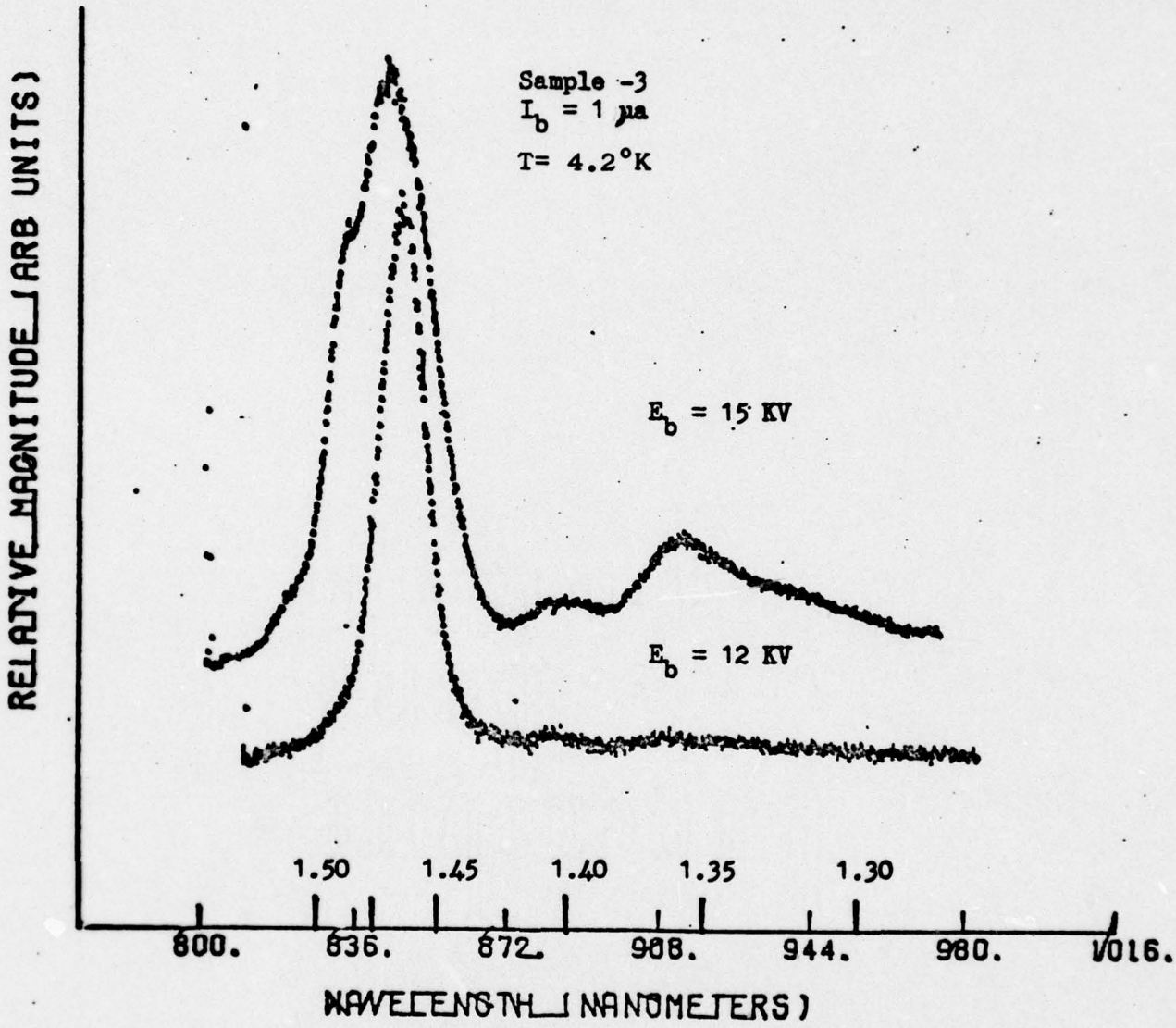

Figure 12. Typical Spectra for Sample Three

Typical spectra for sample four are shown in Figure 13. The 12 KV spectrum consists of five peaks. The peaks at 1.510 eV, 1.404 eV, 1.356 eV, and 1.322 eV are associated with the transitions from sample one with the same energies. The peak at 1.485 eV is associated with the C-C transition. The 15 KV spectrum shows these same four peaks, however, the peak at 1.491 eV is associated with the free-bound carbon acceptor transition.

Depth Related Data

Spectra from sample one recorded at various beam energies are shown in Figure 14. It should be noted that below 10 KV the exciton line at 1.51 eV has disappeared. It should also be noted that the most intense peak below 10 KV is the As vacancy - carbon transition at 1.40 eV.

The free-bound acceptor transition at 1.492 eV is lowered to 1.476 eV in the 8 KV spectrum indicating an acceptor concentration in excess of $5x10^{17}cm^{-3}$. This energy indicates that the acceptor band has moved an additional 16 meV into the band gap.

The C-C line at 1.485 eV has been lowered to 1.445 eV at 8 KV. This indicates a shift of 40 meV. Sixteen meV of this shift is due to the rise of the acceptor band into the gap.

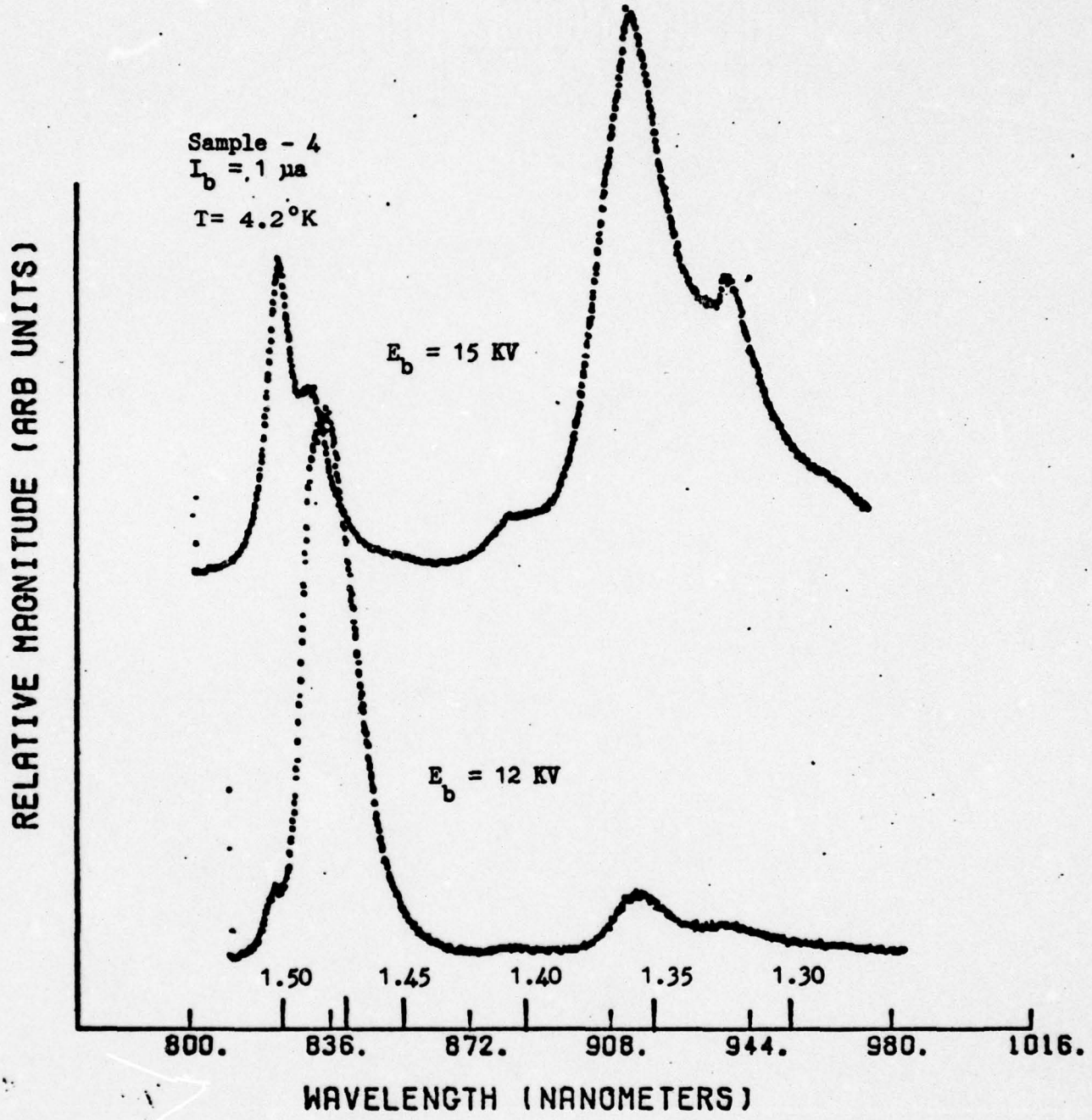

Figure 13. Typical Spectra for Sample Four

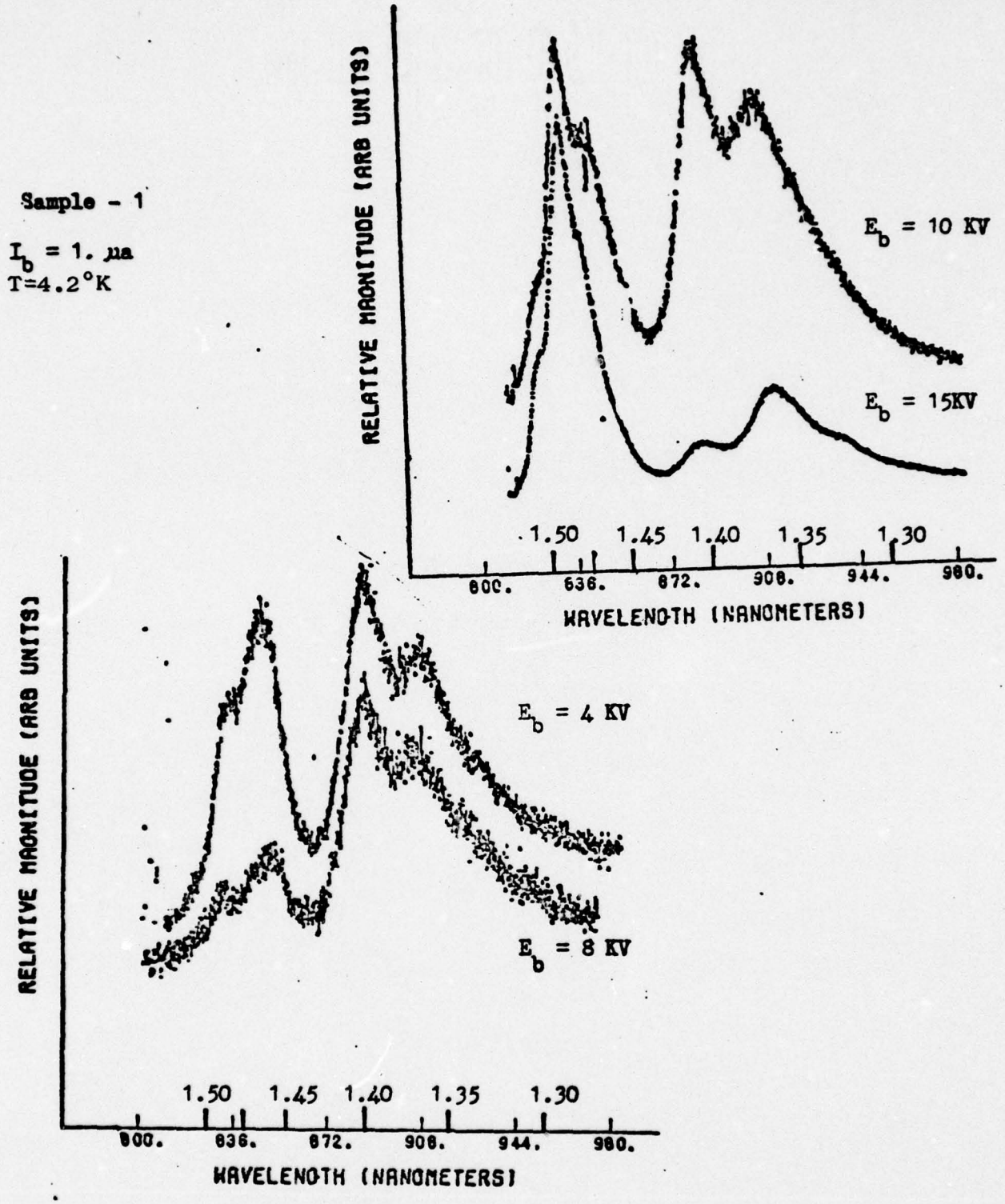

Figure 14. Depth Resolved Spectra for Sample One

The remainder is due to the rise of the donor band into the gap. Since the free-bound acceptor transition is still visible, it appears that the donor level has not merged with the conduction band. Since the bottom of the donor band is 24 meV below the donor level in a lightly doped sample and the donor band is not merged with the conduction band which is 8 meV above the donor level, apparently, the donor band has not banded symmetrically. It appears that the top of the donor band has not shifted as far from the donor level as has the bottom of the band.

Because the donor level has banded but has not merged with the conduction band, the donor concentration is probably between $5x10^{16}$ and $1x10^{17}$ cm^{-3}. This concentration continues to be present even in the 15 KV spectra, though it is obviously not as great further into the material.

The As vacancy - carbon transition also shows a significant shift near 8 KV. This is attributed to the acceptor level rise indicated by the 1.49 eV peak shift.

Spectra from sample 2, recorded at various beam energies, are shown in Figure 15. In these spectra,as in those of sample one, the exciton transition at 1.51 eV disappears below 10 KV. The 1.33 eV peak is also absent. The most intense peak below 10 KV is the C-C peak followed by the free-bound gallium vacancy.

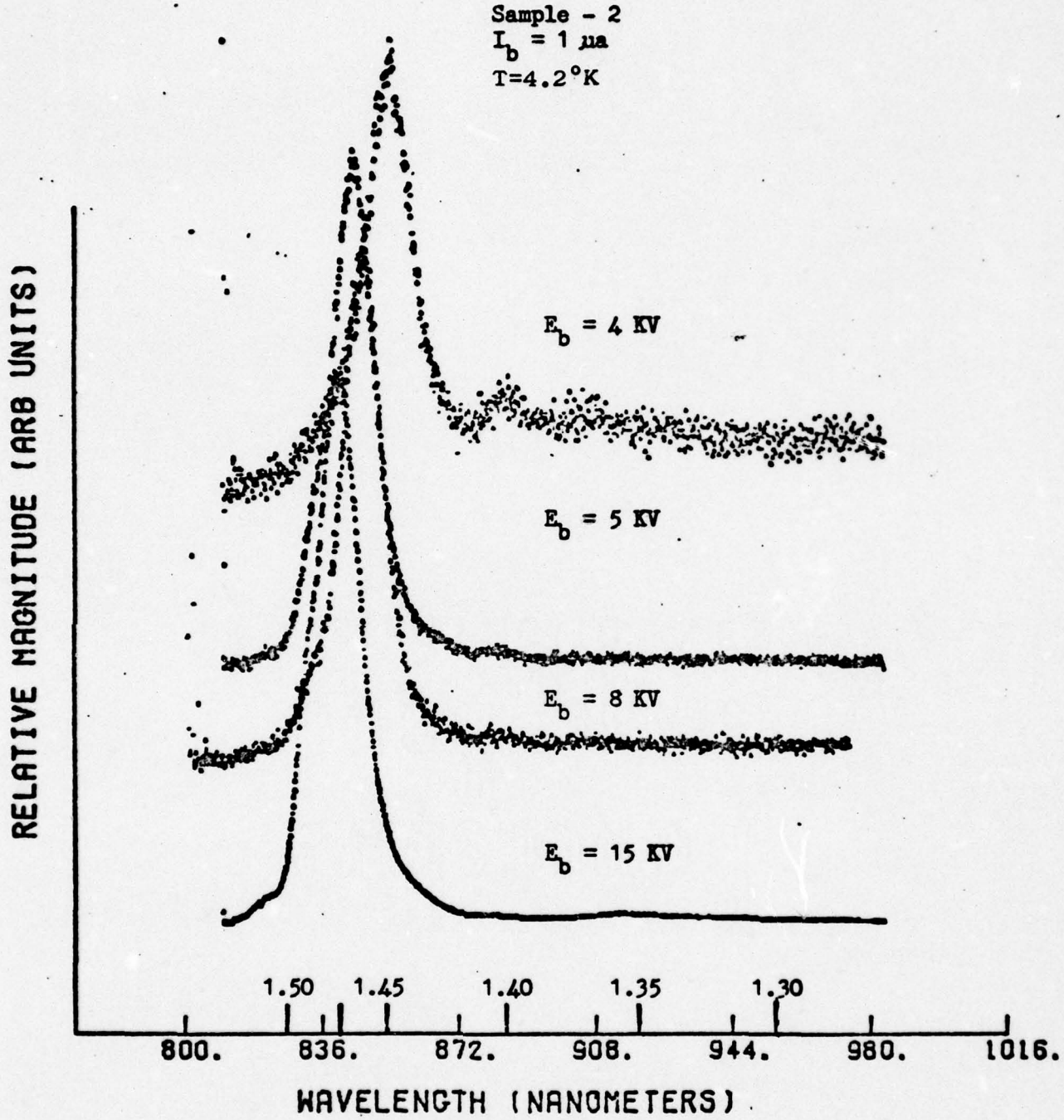

Figure 15. Depth Resolved Spectra for Sample Two

The free-bound acceptor peak is lowered to 1.488 eV indicating a banding in the acceptor level. This peak completely disappears in the 4 KV spectrum indicating the donor band has merged with the conduction band.

The C-C peak shows that banding of the donor level has occured in the 17 KV spectrum some 5 meV below the 1.485 eV donor - acceptor pair value. At 8 KV, where the exciton line has disappeared, it is some 20 meV below. 4 meV of this is due to the acceptor band rise. In the 4 KV spectrum it is lowered some 33 meV and the free-bound acceptor line is not visible. This indicates the merger of the donor band with the conduction band and a concentration in excess of $1x10^{17}cm^{-3}$ donors. The plateau on the high energy side is characteristic of high concentrations. The 17 KV spectra indicates a concentration of greater than $5x10^{16}cm^{-3}$.

Spectra from sample 3 are shown in Figure 16 for various beam energies. The most dominant peak is the C-C transition. The free-bound gallium vacancy transition is also prominant. The exciton line disappears at energies lower than 15 KV as does the free-bound carbon acceptor peak. The carbon acceptor peak shows acceptor level banding at 17 KV and the banding increases till the peak disappears at energies below 15 KV.

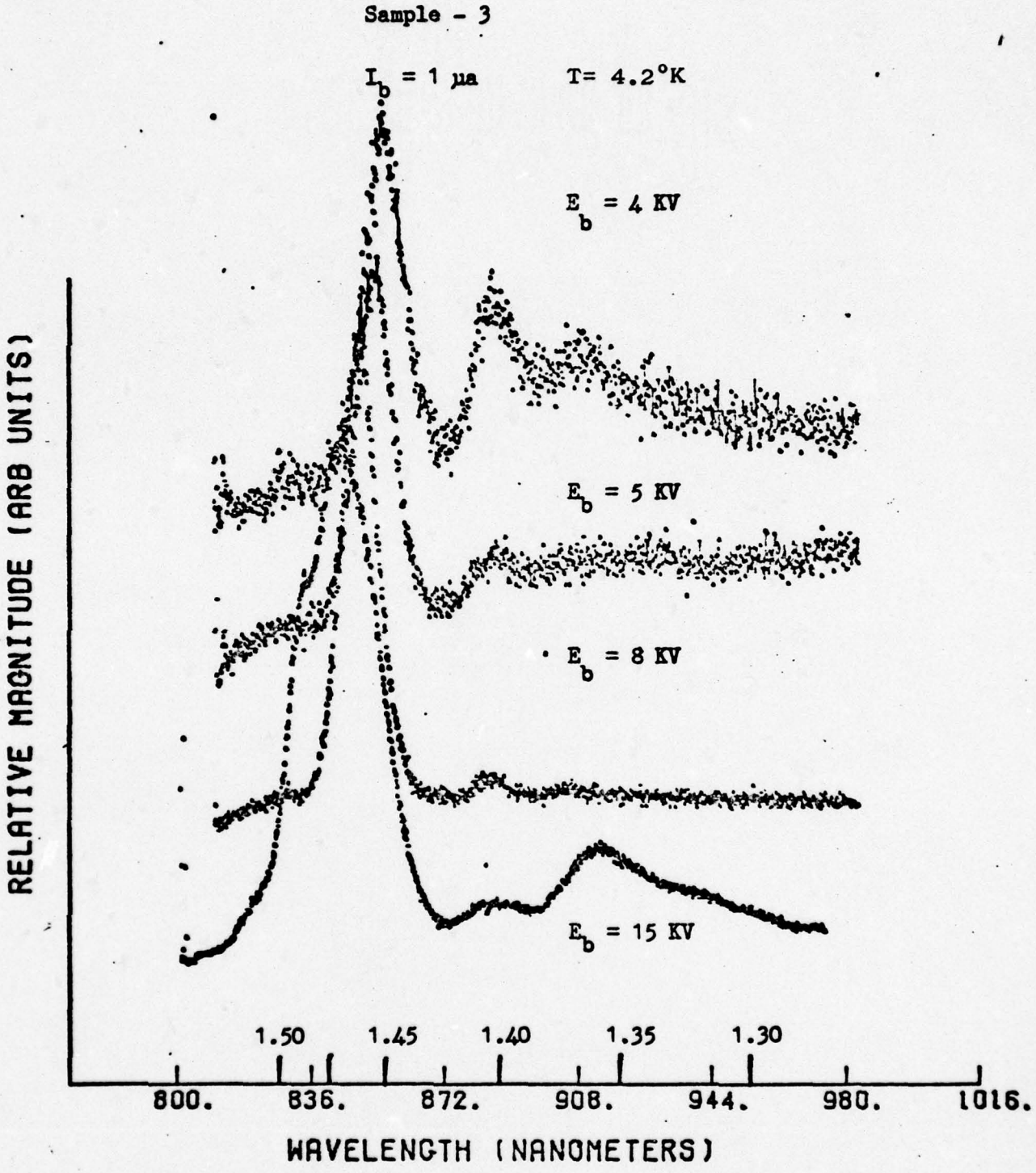

Figure 16. Depth Resolved Spectra for Sample Three

At 15 KV it has moved some 9 meV farther into the gap. The C-C line at this point has been lowered some 16 meV as the donor band has moved 7 meV into the gap. This transition continues to dominate and reduce in energy to the 4 KV spectrum where it is 35 meV below the energy of the donor-acceptor transition in lightly doped material.

The 1.40 eV As vacancy - acceptor transition does not shift appreciably, but exists in all the spectra.

Spectra from sample four at various beam energies are shown in Figure 17. The most dominant peaks in the 15 KV spectrum are the exciton transition and the free-bound Ga vacancy transition. At lower energies the C-C peak dominates. The free-bound acceptor transition and the C-C transition are not resolved in the 10 and 12 KV spectra.

Below 8 KV, the exciton line at 1.51 eV is not visible, while the acceptor transition which shows no banding at this point also disappears. This would indicate an acceptor concentration below $5 \times 10^{17} cm^{-3}$. The C-C transition appears and starts banding near 12 KV. Since the acceptor level transition disappears at 5 KV, it seems the donor band has merged with the conduction band. In the 4 KV spectrum, the C-C line has shifted by some 19 meV and shows the high concentration plateau, where in the 5 KV spectra the shift is only 11 meV.

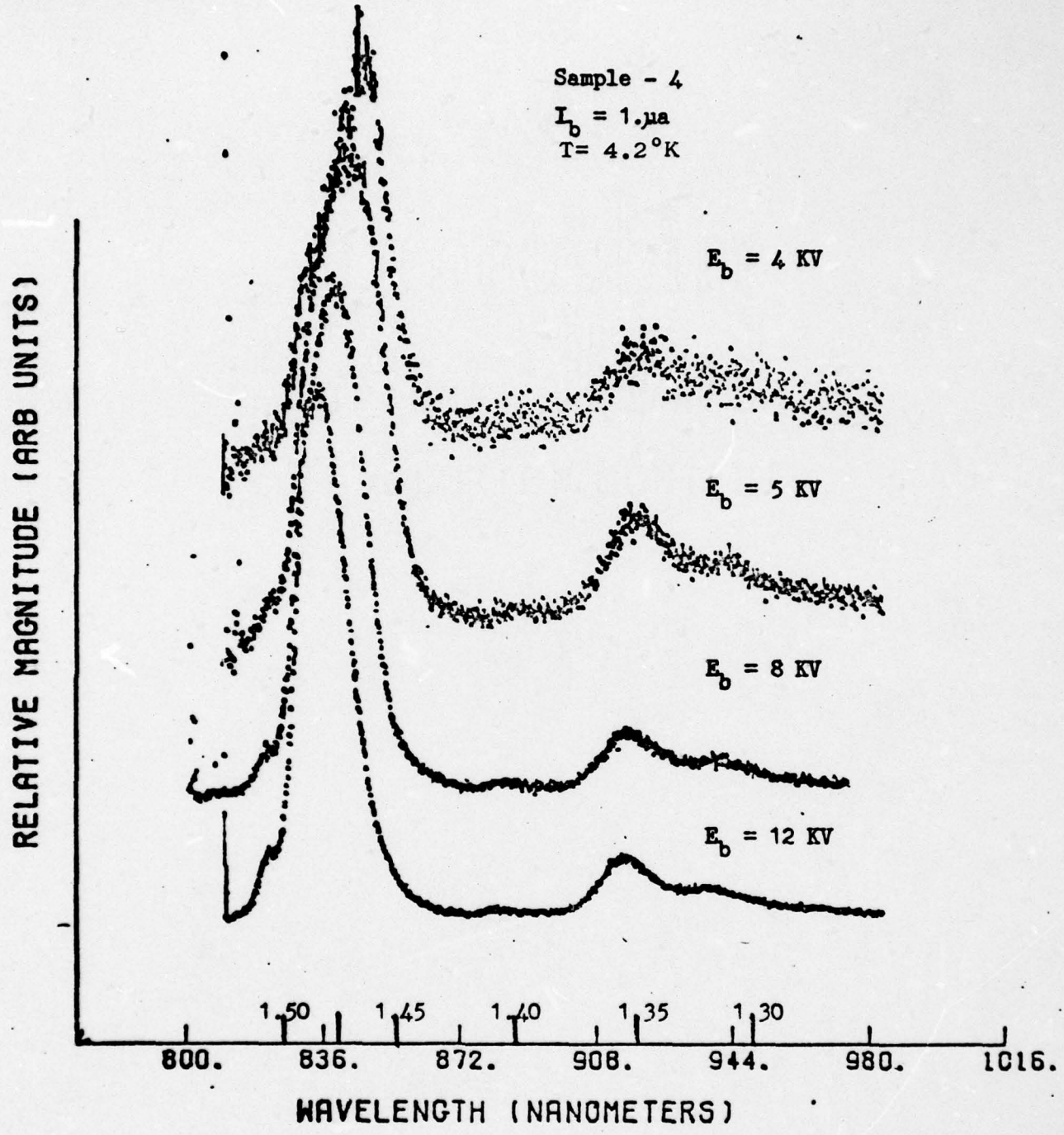

Figure 17. Depth Resolved Spectra for Sample Four

The As vacancy-C line, though never very strong, disappears with the exciton line. The Ga vacancy free-bound transition, which is very strong at high beam energies, is not extinguished even at low beam energies, and shows a slight shift to lower energies.

Concentration of Carbon

In this section, specific concentration levels of carbon as a donor and an acceptor will be inferred from spectra at various beam energies for the four samples. General trends for the carbon concentrations will be discussed by relating luminescence peak energy shift to concentration.

In sample one the acceptor concentration exceeds $5x10^{17}$ cm^{-3} in the 8 KV where it is a maximum. The donor concentration is in excess of $5x10^{16}cm^{-3}$ for energies above 15 KV and is maximized near 8 KV, but does not exceed $1x10^{17}cm^{-3}$.

In sample two the acceptor concentration exceeds $5x10^{17}cm^{-3}$ inside 15 KV. The donor concentration is in excess of $5x10^{16}cm^{-3}$ at 17 KV and exceeds $1x10^{17}cm^{-3}$ at 4 KV.

In sample three the acceptor concentration exceeds $5x10^{17}$ cm^{-3} at 17 KV. Likewise the donor concentration exceeds $5x10^{16}cm^{-3}$ in this spectrum. The donor concentration exceeds $1x10^{17}cm^{-3}$ at 12 KV.

In sample four the acceptor concentration does not exceed $5x10^{17}cm^{-3}$ past the 8 KV spectra. However, the donor concentration exceeds $5x10^{16}cm^{-3}$ at 10 KV and $1x10^{17}cm^{-3}$ at 5 KV.

General trends for the concentration profile can be seen more readily in Figure 18 where the transition energy for the C-C and the free-bound carbon transitions as a function of the electron beam energies. The shift of peak energy to lower values indicates a higher concentration.

In sample one the donor and acceptor concentrations are a maximum at the 8 KV level and a dramatic shift occurs before 10 KV.

In sample two the acceptor concentration does not shift much but the donor concentration shows a drastic change between 4 and 10 KV. Both concentrations decrease with increasing beam energy.

In sample three the acceptor concentration shows a slight shift but the donor concentration shows an increase with energy, the C-C transition changing by 23 meV from 4 to 17 KV.

In sample four the acceptor free-bound transition shows little change while the C-C transition shift indicates a substantial rise fom 4 to 12 KV.

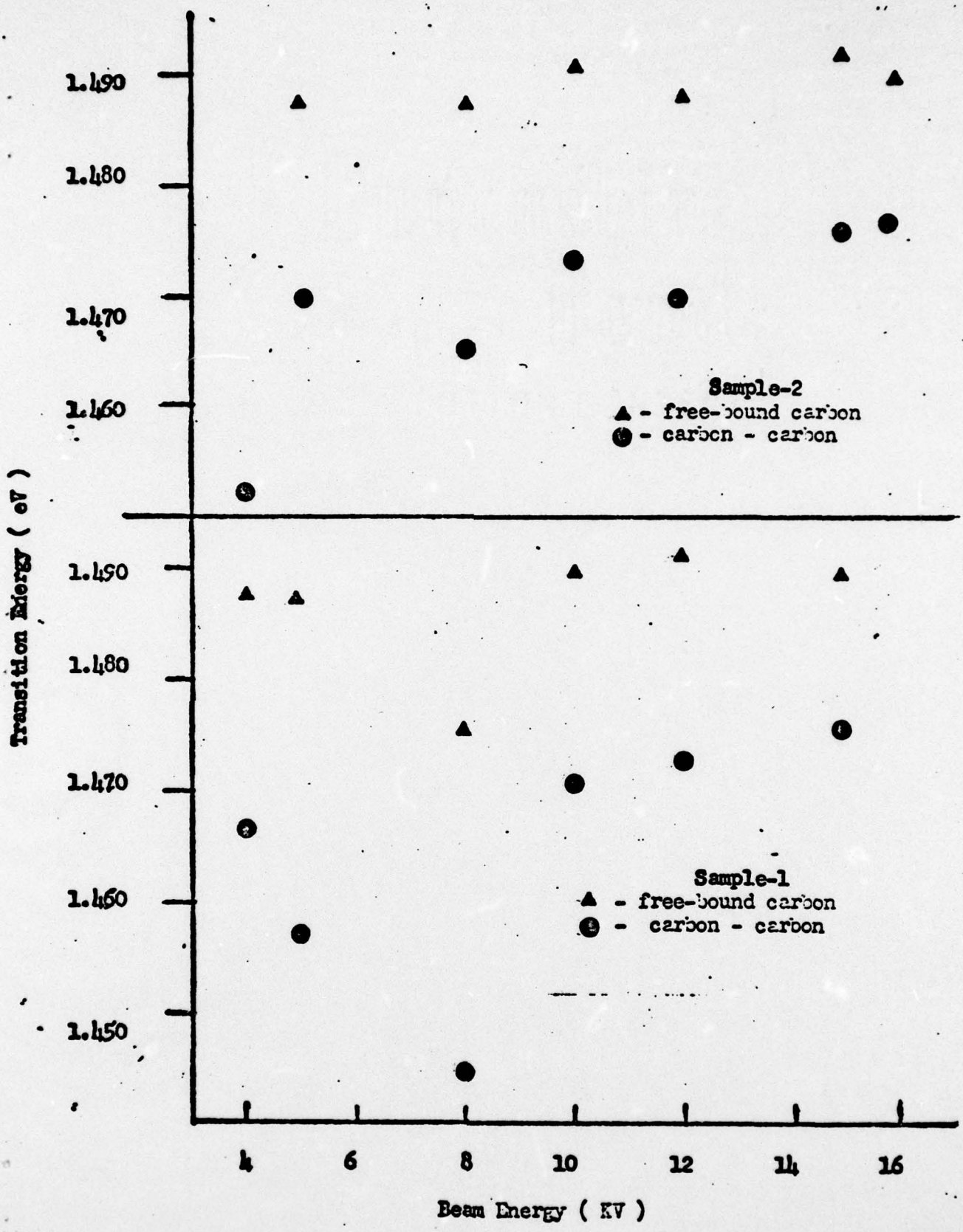

Figure 18. Variation of Transition Energy with Beam Energy

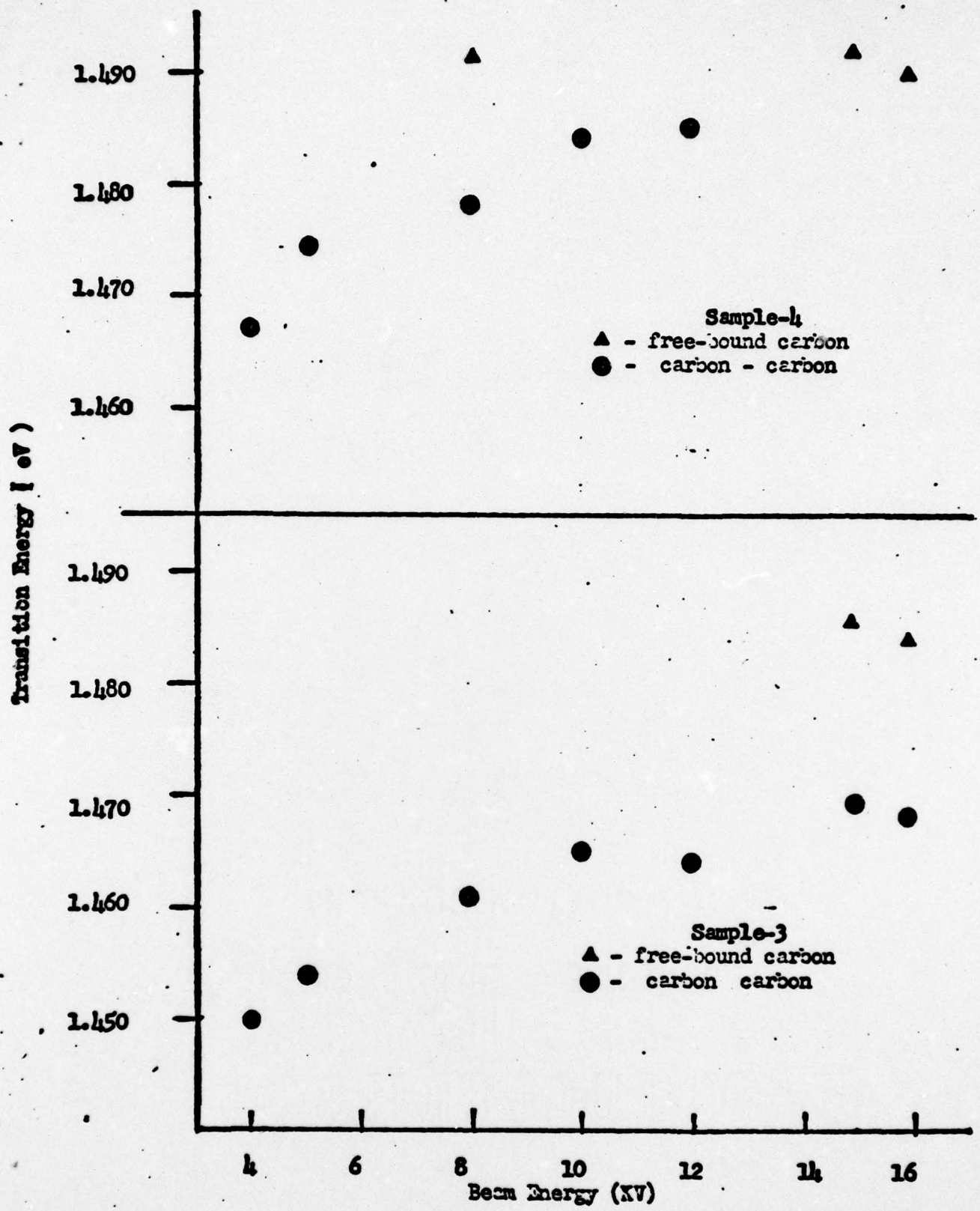

Figure 18 (cont.) Variation of Transition Energy with Beam Energy

Effects of Different Capping Methods

Since samples one and two were prepared from the same implanted wafer differences in their depth resolved luminescence must be due to the annealing with differenct caps as the implant profile before annealing should be the same. It should be noted though that penetration of the Si_3N_4 cap requires a KV more energy than the SiO_2 cap.

Spectra from these two crystals are compared at 8 and 12 KV in Figures 19 and 20. At 8 KV the spectra of the SiO_2 capped sample is dominated by the C-C transition and shows a very weak As vacancy - carbon peak. On the other hand, a strong As vacancy - carbon peak is found in the Si_3N_4 capped crystal. The free-bound Ga vacancy is also prominent.

The shift in the C-C peak energy indicates a low donor concentration in the Si_3N_4 capped sample as opposed to the SiO_2 capped sample. This would indicate a larger outflux of Ga from the SiO_2 capped crystal.

The shift of the free-bound carbon peak in the Si_3N_4 capped crystal indicates a larger acceptor concentration than in the SiO_2 capped crystal. With this, the As vacancy - carbon peak is very strong indicating a larger outflux of As through the Si_3N_4 cap.

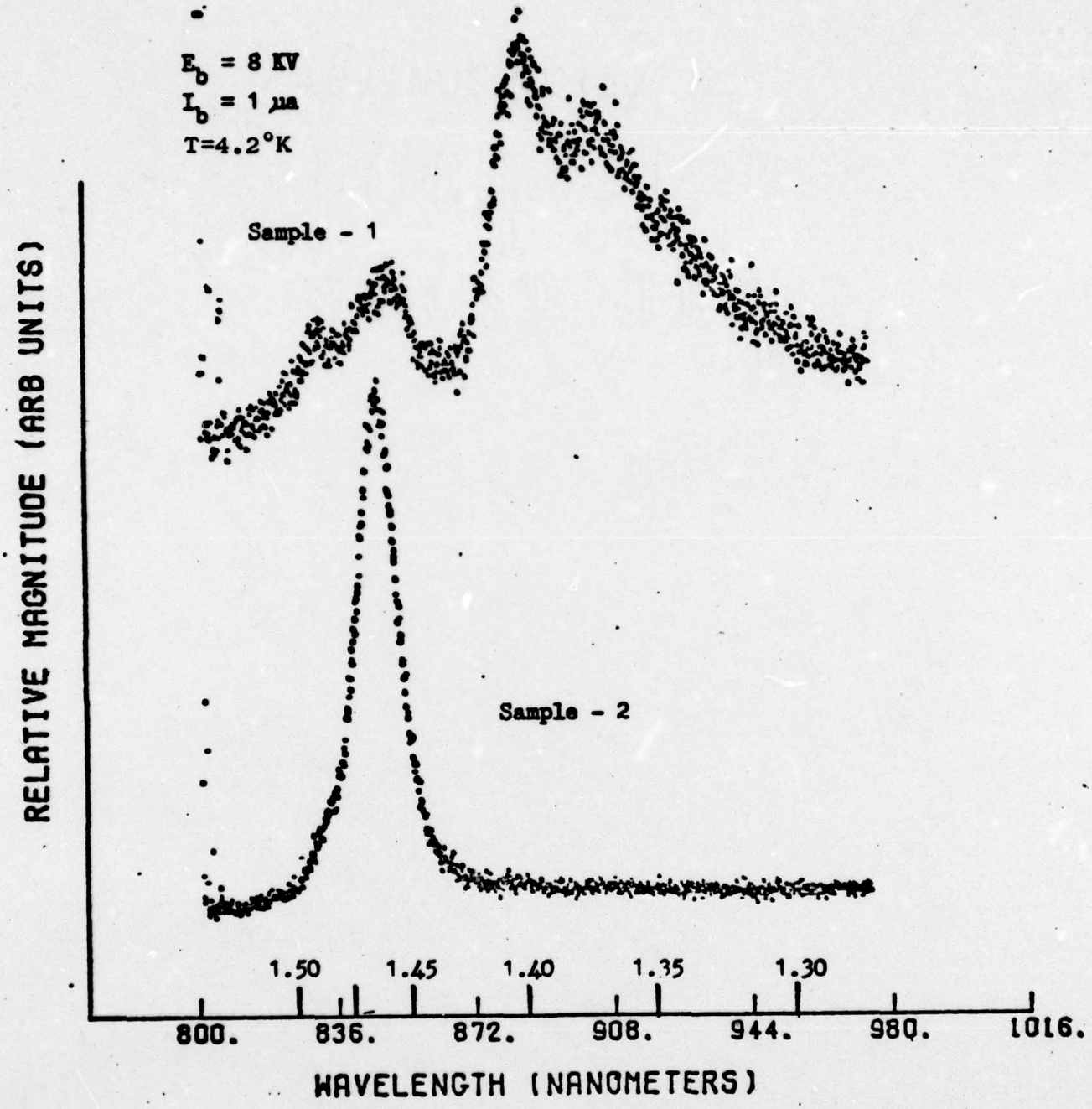

Figure 19. Capping Effects for 8 KV Beam

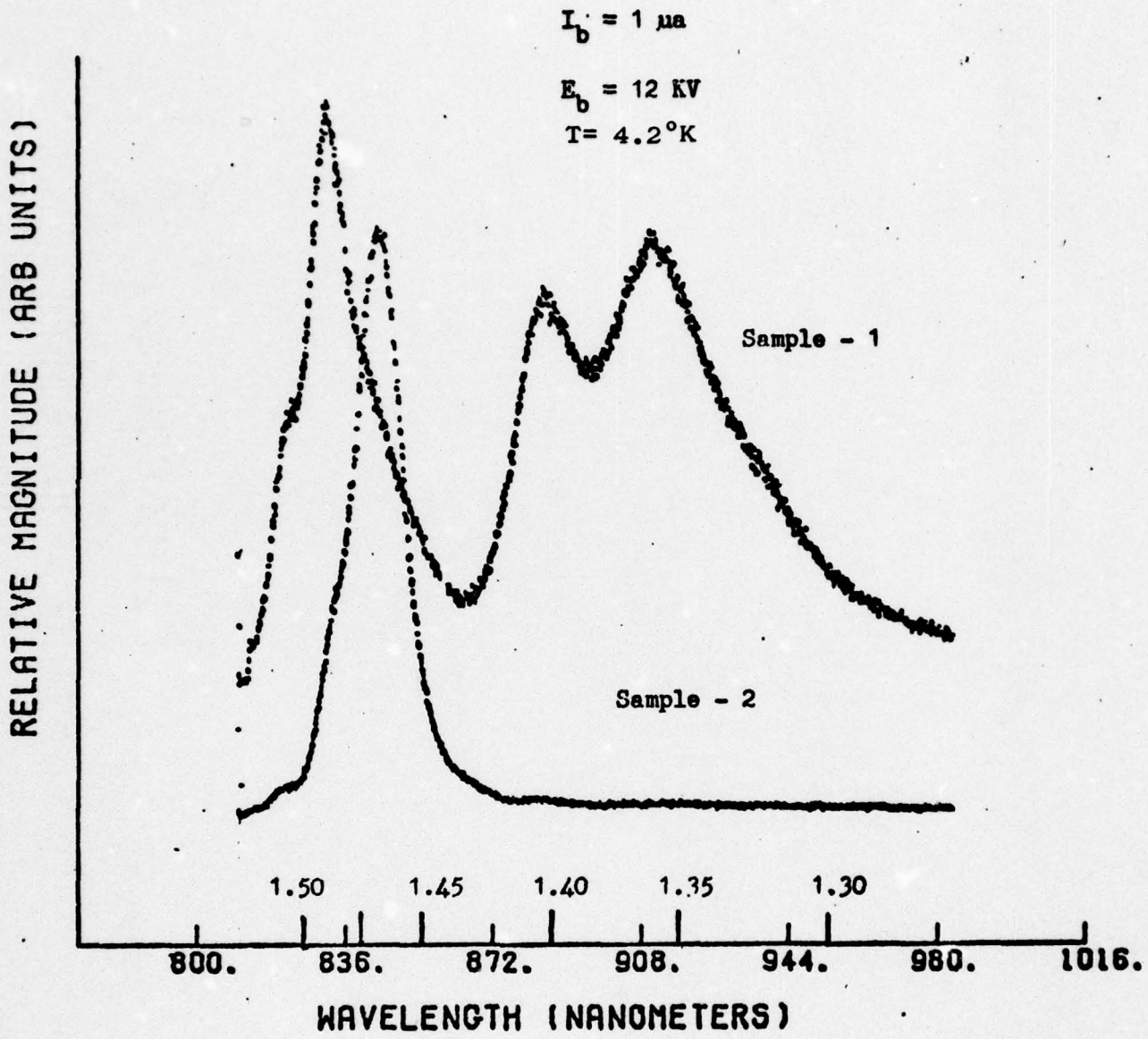

Figure 20. Capping Effects for 12 KV Beam

The spectra of sample three is dominated by the C-C transition. Vacancy associated peaks are small and most intense farther into the material, where the free-bound Ga vacancy is the most prominent of them. This would indicate that the carbon ions are substituting substitutionally for vacancies which should be more dominanant near the surface where outdiffusion would be more prominent.

V. CONCLUSIONS

The luminescence peak which shifts in energy more than the others, and is the most prominent near the surface for three of the four samples has been identified as the C-C transition. This would indicate that the carbon is substituting for both Ga and As.

Since the SiO_2 capped sample does not exhibit the free-bound carbon acceptor peak at low energy while the Si_3N_4 capped sample does, would indicate a higher concentration of carbon donors in the SiO_2 capped sample and a higher Ga outdiffusion through SiO_2 than Si_3N_4.

The greater shift in the carbon free-bound acceptor transition and the presence of this peak in all spectra for the Si_3N_4 capped sample as well as the prominance of the As vacancy carbon acceptor transition would indicate a higher acceptor concentration in Si_3N_4 capped sample than the SiO_2 capped sample, and hence a greater outdiffusion of As through the Si_3N_4 than the SiO_2.

The $10^{14}cm^{-2}$ fluence reduced the intensity of the vacancy associated peaks which would indicate a higher number of substitutional carbons than in the $10^{13}cm^{-2}$ fluence. The carbon profile tailed much farther into the crystal with the higher fluence than with the lower fluence.

BIBLIOGRAPHY

1. Ashen, D.J. et al, "The Incorporation and Characterization of Acceptors in Epitaxial GaAs," Journal of Physics and Chemistry of Solids, 36: 1041 (1975).

2. Bebb, H.B. and E.W. Williams. "Photo-luminescence I: Theory," Semiconductors and Semimetals, Vol. VIII; 182 (1972).

3. Bogardus, E.H. and H.B. Bebb. "Bound Exciton, Free Exciton, Band-Acceptor, Donor-Acceptor and Auger Recombinations in GaAs," Physical Review, 176: 993-1002 (December 1968).

4. Boulet, D.L. Depth Resolved Cathodoluminescence of Cadmium Implanted Gallium Arsenide, Unpublished Thesis, Wright-Patterson Air Force Base, Ohio: Air Force Institute of Technology (December 1975).

5. Chatterjee, P.K., et al. "Photoluminescence Study of Native Defects in Annealed GaAs," Solid State Communications, 17: 1421-4 (1975).

6. Cusano, D.A. "Radiative Recombination From GaAs Directly Excited by Electron Beams," Solid State Communications, 2: 353-8 (1964).

7. Dean, P.J. "Junction Electroluminescence," Applied Solid State Science, 1: 1-151 (1969).

8. Dumoulin, J.D. Depth Resolved Cathodeluminescence on the Effects of Cd Implantation and Annealing in Gallium Arsenide, Unpublished thesis, Wright-Patterson Air Force Base, Ohio: Air Force Institute of Technology (December 1976).

9. Gibbons, J.F. "Ion Implantation in Semiconductors - Part I Range Distribution Theory and Experiments," Proceedings of the IEEE, 56: 295-8 (March 1968).

10. Itoh, T and M. Takeuchi. "Arsenic Vacancy Formation in GaAs Annealed in Hydrogen Flow," Japanese Journal of Applied Physics, 16: 227-32 (February 1977).

11. Kamiya, T. and E. Wagner. "Shallow Acceptor Binding Energy and Lifetime of Donor-Acceptor Pairs in Gallium Arsenide," Journal of Applied Physics, 47: 3219-23 (July 1976).

12. Marcyk, G.T. Glow Discharge Optical Spectroscopy for Measurements of Boron Implanted Distributions in Silicon, Unpublished thesis, Urbana Illinois, University of Illinois at Urbana - Champaign (1976).

13. Martinelli, R.U. and C.C. Wang. "Electron Beam Penetration in GaAs," Journal of Applied Physics, 44: 3350-1 (July 1973).

14. McKelvey, J.P. Solid State and Semiconductor Physics, New York: Harper and Row (1966).

15. Norris, C.B. et al. "Depth-Resolved Cathodoluminescence in Undamaged and Ion Implanted GaAs, ZnS, and CdS," Journal of Applied Physics, 44: 3209-3221 (July 1973).

16. Pankove, J.I. Optical Processes in Semiconductors, Englewood Cliffs, New Jersey: Prentice-Hall (1971).

17. Pierce, B.J. Time Resolved Spectroscopy of ZnSe, Unpublished thesis, Wright-Patterson Air Force Base, Ohio: Air Force Institute of Technology (June 1969).

18. ..... Luminescence and Hall Effect of Ion Implanted Layers in ZnO, Unpublished thesis, Wright-Patterson Air Force Base, Ohio: Air Force Institute of Technology (September 1974).

VITA

PII Redacted

Martin J. Walter was born on [redacted], the son of [redacted]. Upon graduation from Akron Kenmore High School in 1972, Martin attended the University of Akron, in Akron, Ohio. In June of 1976 he was awarded the degree of Bachelor of Science in Physics and a commission in the United States Air Force. Lt Walter was assigned to the Air Force Institute of Technology in August 1976.

PII Redacted

Permanent Address: [redacted]

This thesis was typed by Ms. Sherry Markiewicz.

UNCLASSIFIED

SECURITY CLASSIFICATION OF THIS PAGE (When Data Entered)

REPORT DOCUMENTATION PAGE		READ INSTRUCTIONS BEFORE COMPLETING FORM
1. REPORT NUMBER AFIT/GEP/PH/77-15	2. GOVT ACCESSION NO.	3. RECIPIENT'S CATALOG NUMBER
4. TITLE (and Subtitle) DEPTH RESOLVED CATHODOLUMINESCENCE OF CARBON IMPLANTED GALLIUM ARSENIDE		5. TYPE OF REPORT & PERIOD COVERED MS THESIS
		6. PERFORMING ORG. REPORT NUMBER
7. AUTHOR(s) MARTIN J. WALTER 2Lt. ,USAF		8. CONTRACT OR GRANT NUMBER(s)
9. PERFORMING ORGANIZATION NAME AND ADDRESS Air Force Institute of Technology (AFIT-EN) Wright-Patterson AFB, Ohio 45433		10. PROGRAM ELEMENT, PROJECT, TASK AREA & WORK UNIT NUMBERS
11. CONTROLLING OFFICE NAME AND ADDRESS		12. REPORT DATE December, 1977
		13. NUMBER OF PAGES 65
14. MONITORING AGENCY NAME & ADDRESS(if different from Controlling Office)		15. SECURITY CLASS. (of this report) Unclassified
		15a. DECLASSIFICATION/DOWNGRADING SCHEDULE

16. DISTRIBUTION STATEMENT (of this Report)

Approved for public release; distribution unlimited

17. DISTRIBUTION STATEMENT (of the abstract entered in Block 20, if different from Report)

18. SUPPLEMENTARY NOTES

Approved for public release; IAW AFR 190-17

JERRAL F. GUESS, Captain, USAF
Director of Information

19. KEY WORDS (Continue on reverse side if necessary and identify by block number)

CATHODOLUMINESCENCE
GALLIUM ARSENIDE
ION-IMPLANTATION
LUMINESCENCE
SPECTRA

20. ABSTRACT (Continue on reverse side if necessary and identify by block number)

The effects of two caps, SiO_2 and Si_3N_4, are examined on Cr doped GaAs by means of depth resolved Cathodoluminescence. The GaAs samples had been implanted with C in fluences of 10^{13} cm^{-2} and 10^{14} cm^{-2}. Two of the samples differed only in the cap used.

The energy shift in the carbon-carbon, donor-acceptor, recombination, and the free-bound, carbon acceptor transition peak are used to evaluate the carbon donor, and carbon acceptor concentrations. These concentrations

DD FORM 1 JAN 73 1473 EDITION OF 1 NOV 65 IS OBSOLETE

UNCLASSIFIED

SECURITY CLASSIFICATION OF THIS PAGE (When Data Entered)

10 to the -13th power/sq cm and 10 to the -14th power/sq cm

are used to evaluate the effects of the caps.

It is found that the carbon substitutes for both Ga and As; and that the Si_3N_4 cap permits greater outdiffusion of As than the SiO_2 cap; and that the SiO_2 cap permits greater outdiffusion of the Ga than does the Si_3N_4 cap.